Physica Scripta

PAPER

An efficient semi-analytical techniques for the fractional-order system of Drinfeld-Sokolov-Wilson equation

Abdul Hamid Ganie[1], **Humaira Yasmin**[2,*], **A A Alderremy**[3], **Rasool Shah**[4,*] **and Shaban Aly**[5]

[1] Basic Science Department, College of Science and Theoretical Studies, Saudi Electronic University, Riyadh 11673, Saudi Arabia
[2] Department of Basic Sciences, General Administration of Preparatory Year, King Faisal University, Al-Ahsa, 31982, Saudi Arabia
[3] Department of Mathematics, Faculty of Science, King Khalid University, Abha 61413, Saudi Arabia
[4] Department of Computer Science and Mathematics, Lebanese American University, Beirut Lebanon
[5] Department of Mathematics, Faculty of Science, AL-Azhar University, Assiut, Egypt
[*] Authors to whom any correspondence should be addressed.

E-mail: a.ganie@seu.edu.sa, hhassain@kfu.edu.sa, aaldramy@kku.edu.sa, rasool.shah@lau.edu.lb **and** shhaly70@yahoo.com

Keywords: Drinfeld-Sokolov-Wilson system, Aboodh transform iteration method, Aboodh residual power series method, fractional order differential equation, Caputo operator

OPEN ACCESS

RECEIVED
5 November 2023

REVISED
3 December 2023

ACCEPTED FOR PUBLICATION
20 December 2023

PUBLISHED
2 January 2024

Abstract

This study delves into the exploration and analysis of the fractional order Drinfeld-Sokolov-Wilson (FDSW) system within the framework of the Caputo operator. To address this complex system, two innovative methods, namely the Aboodh transform iteration method (ATIM) and the Aboodh residual power series method (ARPSM), are introduced and applied. These methods offer efficient computational tools to investigate the FDSW system, particularly in the fractional order context utilizing the Caputo operator. The ATIM and ARPSM are employed to solve and analyze the FDSW system, allowing for the derivation of solutions and insights into the system's behavior and dynamics. The utilization of these novel methods showcases their efficacy in handling the intricate characteristics of the FDSW system under fractional differentiation, offering a deeper understanding of its mathematical properties and behaviors.

1. Introduction

Fractional calculus finds diverse applications across numerous scientific and engineering fields. Complex systems with memory and non-local behavior may now be modeled and analyzed with its help. In control theory, for instance, it is essential in planning systems with complex dynamics. Fractional calculus is also important in signal processing because it helps to explain and control signals that exhibit fractal-like behavior. It's useful in material science for characterizing viscoelastic materials, which may behave both like solids and liquids [1–5]. Its adaptability and importance in solving a broad variety of real-world issues is further shown by its applicability to fields as diverse as electrochemistry, medicine, finance, and geophysics [6–12]. Classical derivatives have a local character, allowing us to evaluate changes in the vicinity of a point, whereas Caputo fractional derivatives have a nonlocal nature, allowing us to analyze changes in an interval. This trait makes the Caputo fractional derivative applicable to modeling a wider variety of physical phenomena, including ocean climate, atmospheric physics, dynamical systems, earthquakes, vibrations, polymers, etc (refer to the scholarly literature cited in [13–18] for additional details).

Here, in our present study, we start by examining the Drinfeld-Sokolov-Wilson system provided by

$$\frac{\partial}{\partial \epsilon}\varphi_a(\eta,\,\epsilon) + 3\varphi_b(\eta,\,\epsilon)\frac{\partial \varphi_b(\eta,\,\epsilon)}{\partial \eta} = 0,$$

$$\frac{\partial}{\partial \epsilon}\varphi_b(\eta,\,\epsilon) + 2\frac{\partial^3 \varphi_b(\eta,\,\epsilon)}{\partial \eta^3} + 2\varphi_a(\eta,\,\epsilon)\frac{\partial \varphi_b(\eta,\,\epsilon)}{\partial \eta} + \varphi_b(\eta,\,\epsilon)\frac{\partial \varphi_a(\eta,\,\epsilon)}{\partial \eta} = 0,$$

subject to the initial condition:

$$\varphi_a(\eta, 0) = Q_{a0}(\eta),$$
$$\varphi_b(\eta, 0) = R_{b0}(\eta).$$

Exact solution given in [19] as:

$$\varphi_a(\eta, \epsilon) = \frac{3c}{2}\,\mathrm{sech}^2\left(\sqrt{\frac{c}{2}}(\eta - c\epsilon)\right),$$
$$\varphi_b(\eta, \epsilon) = c\,\mathrm{sech}\left(\sqrt{\frac{c}{2}}(\eta - c\epsilon)\right).$$

The nonlinear Drinfeld-Sokolov-Wilson (DSW) model is a fundamental mathematical model in mathematical physics [19–22]. It has applications in a variety of fields, including fluid dynamics, plasma physics, geochemistry, astrophysics, chemical kinematics, chemical chemistry, solid state physics, and optical fiber. Several scientists and mathematicians have recently studied the DSW equation in both fractional and integer orders [27–30]. Wave packets that travel in a nonlinear dispersive medium are known as solitary waves. Notable scholars like Abdulloev *et al* [23], Bona *et al* [24], etc have written work in this area. These mathematical models are also crucial for studying shallow water waves, ion-acoustic plasma waves, and nonlinear dispersive waves [25, 26]. In a recent publication, Yang [31] defined and proposed generalized fractional operators and their applications in engineering and research. A unique fractional operator with a non-singular kernel was proposed by Yang *et al* [32] and its applications in the study of constant heat flow were suggested. Another novel fractional derivative with a non-singular kernel for the normalized sinc function was introduced by Yang *et al* [33, 34] found solution to problem in the exponential decay kernel of models of anomalous diffusion. Nonlinear differential equations with a fractional derivative, power, and a Mittag-Leffler kernel were numerically solved by Yepez-Martinez and Gomez-Aguilar [35]. The numerical approximation of the Riemann-Liouville definition of a fractional operator was provided by Atangana and Gomez-Aguilar [36]. In order to manage linear partial differential equations with a fractional operator connected with a non-singular kernel, Morales-Delgado *et al* [37] used the Laplace homotopy analysis method. Fractional operators with the no-index law property were used to chaos theory and statistical analysis by Atangana and Gomez-Aguilar [38]. For the time-fractional Korteweg–de Vries problem, Yokus [39] used the finite difference approach to evaluate the Caputo and conformable operators.

The fractionalized DSW equation may be written as:

$$D_\epsilon^p \varphi_a(\eta, \epsilon) + 3\varphi_b(\eta, \epsilon)\frac{\partial \varphi_b(\eta, \epsilon)}{\partial \eta} = 0,$$
$$D_\epsilon^p \varphi_b(\eta, \epsilon) + 2\frac{\partial^3 \varphi_b(\eta, \epsilon)}{\partial \eta^3} + 2\varphi_a(\eta, \epsilon)\frac{\partial \varphi_b(\eta, \epsilon)}{\partial \eta} + \varphi_b(\eta, \epsilon)\frac{\partial \varphi_a(\eta, \epsilon)}{\partial \eta} = 0, \quad \text{where} \quad 0 < p \leqslant 1$$

Omar Abu Arqub, a mathematician from Jordan, created the residual power series method (RPSM) in 2013 [40]. The RPSM is a semi-analytical method that combines the residual error function with Taylor's series. The offered convergence series techniques may be used to solve both linear and nonlinear DEs. The first time RPSM was used to fuzzy DE resolution was in 2013. Arqub *et al* [41] created a unique set of RPSM algorithms to effectively get power series solutions for extensive DEs.Fractional order non-linear boundary value problems are also addressed by a novel and appealing RPSM method developed by Arqub *et al* [42]. To approximate solutions to KdV-burgers equations of fractional order, El-Ajou *et al* [43] devised a unique RPSM iterative approach.It was first proposed by Xu *et al* [44] initially proposed utilizing fractional power series solutions to solve second- and fourth-order Boussinesq differential equations (DEs). By combining RPSM with least square methods, Zhang *et al* [45] developed a robust numerical approach (For more detail see [46–48]).

Two reliable methods were used by the researchers to tackle fractional-order differential equations (FODEs). This new method, which is a hybrid of the Sumudu transform and the homotopy perturbation technique [49], works by first mapping the initial equation onto the space of the Aboodh transform, then finding a series of solutions for the modified form of the equation, and finally finding the solution to the original equation via the inverse Aboodh transform. The unique technique generates solutions for linear and nonlinear PDEs using power series expansions, eliminating the need for linearization, perturbation, or discretization. In contrast to RPSM, which needs a large number of iterations during the solution phases to compute different fractional derivatives, finding the coefficients involves just a small number of calculations. The suggested method may provide an approximation solution that is both closed-form and accurate since it uses a quick convergence series.

The solution of fractional partial differential equations via the Aboodh Transform Iterative Method (NITM) stands as a significant mathematical achievement of the past century. Because of their computational complexity

and lack of convergence, partial differential equations with fractional derivatives are famously difficult to solve using traditional methods. In order to get around these limitations, our novel approach continuously improves approximate solutions, thus increasing their precision while reducing the computing weight. This strategy has been demonstrated to enhance solutions for a wide range of difficult mathematical and physical problems by tailoring iterations to the properties of fractional derivatives [50–52]. We can now tackle challenging issues in physics, engineering, and applied mathematics because of the improvements gained in describing and understanding complicated systems governed by fractional partial differential equations. The scientific landscape is a tapestry woven with diverse threads of research spanning various disciplines. The recent publications across multidisciplinary domains reflect the rich tapestry of scientific inquiry. Noteworthy contributions include pioneering studies on manipulating terahertz wavefronts through cascaded metasurfaces [53], the discovery of the first hidden-charm pentaquark with strangeness [54], and investigations into the dynamical properties and chaotic behaviors of nonlinear coupled Schrodinger equations in fiber Bragg gratings [55]. Additionally, innovative methodologies, such as an Iterative Threshold algorithm of Log-Sum Regularization for Sparse Problems [56], and novel control strategies for uncertain nonlinear systems [57], stand as testament to the diverse research endeavors in various scientific domains. Furthermore, pioneering approaches in machinery failure identification [58], threat assessment of aerial targets [59], and their respective methodologies signal the continuous evolution and interdisciplinary nature of scientific exploration across fields like engineering, physics, mathematics, and biosciences.

In order to solve fractional differential equations, two of the simplest methods are the Aboodh residual power series method (ARPSM) [60, 61] and the Aboodh transform iterative method (NITM) [50–52]. These methods offer approximate numerical solutions to both linear and nonlinear differential equations without necessitating linearization or discretization, further providing immediate and observable symbolic terms of analytic solutions. The primary purpose of this research is to apply and compare two distinct approaches, namely ARPSM and NITM, to the solution of the DSW system, a nonlinear partial differential equations. It should be noted that these two approaches have been used to solve a variety of nonlinear fractional differential problems.

2. Basic definitions

Definition 2.1. [62] Let $\varphi(\eta,\ \epsilon)$ is of exponential order and piecewise continuous function. For $\tau \geqslant 0$, the Aboodh transform of $\varphi(\eta,\ \epsilon)$ is define as:

$$A[\varphi(\eta,\ \epsilon)] = \Psi(\eta,\ \nu) = \frac{1}{\nu}\int_0^{\infty} \varphi(\eta,\ \epsilon)e^{-\epsilon\nu}d\epsilon,\ \ r_1 \leqslant \nu \leqslant r_2,$$

We may write the inverse Aboodh transform as:

$$A^{-1}[\Psi(\eta,\ \nu)] = \varphi(\eta,\ \epsilon) = \frac{1}{2\pi i}\int_{u-i\infty}^{u\ +\ i\infty} \Psi(\eta,\ \epsilon)\nu e^{\epsilon\nu}d\epsilon$$

Where $\eta = (\eta_1, \eta_2, \cdots, \eta_p)$ and $p \in \mathbb{N}$

Lemma 2.1. *[63, 64] Let $\varphi_1(\eta,\ \epsilon)$ and $\varphi_2(\eta,\ \epsilon)$ be of exponential order and piecewise continuous on $[0,\ \infty[$. Assume that $A[\varphi_1(\eta,\ \epsilon)] = \Psi_1(\eta,\ \epsilon)$, $A[\varphi_2(\eta,\ \epsilon)] = \Psi_2(\eta,\ \epsilon)$ and $\lambda_1,\ \lambda_2$ are constants. Then the following properties are true:*

1. $A[\lambda_1\varphi_1(\eta,\ \epsilon) + \lambda_2\varphi_2(\eta,\ \epsilon)] = \lambda_1\Psi_1(\eta,\ \nu) + \lambda_2\Psi_2(\eta,\ \nu)$,
2. $A^{-1}[\lambda_1\Psi_1(\eta,\ \epsilon) + \lambda_2\Psi_2(\eta,\ \epsilon)] = \lambda_1\varphi_1(\eta,\ \nu) + \lambda_2\varphi_2(\eta,\ \nu)$,
3. $A[J_\epsilon^p\varphi(\eta,\ \epsilon)] = \frac{\Psi(\eta,\nu)}{\nu^p}$,
4. $A[D_\epsilon^p\varphi(\eta,\ \epsilon)] = \nu^p\Psi(\eta,\ \nu) - \sum_{K=0}^{r-1}\frac{\varphi^K(\eta,0)}{\nu^{K-p+2}},\ r-1 < p \leqslant r,\ r \in \mathbb{N}$.

Definition 2.2. [65] $\varphi(\eta,\ \epsilon)$ of order p has the following definition for its fractional derivative in the Caputo sense:

$$D_\epsilon^p\varphi(\eta,\ \epsilon) = J_\epsilon^{m-p}\varphi^{(m)}(\eta,\ \epsilon),\ r \geqslant 0,\ m-1 < p \leqslant m,$$

where $\eta = (\eta_1,\ \eta_2,\cdots,\eta_p) \in \mathbb{R}^p$ and $m,\ p \in R$, J_ϵ^{m-p} is the R-L integral of $\varphi(\eta,\ \epsilon)$.

Definition 2.3. [66] The power series is shown in the following form:

$$\sum_{r=0}^{\infty} \hbar_r(\eta)(\epsilon - \epsilon_0)^{rp} = \hbar_0(\epsilon - \epsilon_0)^0 + \hbar_1(\epsilon - \epsilon_0)^p + \hbar_2(\epsilon - \epsilon_0)^{2p} + \cdots,$$

where $p \in \mathbb{N}$ and $\eta = (\eta_1, \eta_2, \cdots, \eta_p) \in \mathbb{R}^p$. This kind of series is called multiple fractional power series (MFPS) about ϵ_0, where the series coefficients are $\hbar_r(\eta)'s$ and ϵ indicates a variable.

Lemma 2.2. *Let us assume that $\varphi(\eta, \epsilon)$ is an exponentially ordered function. Subsequently, $A[\varphi(\eta, \epsilon)] = \Psi(\eta, \nu)$ represents the Aboodh transform. Hence,*

$$A[D_\epsilon^{rp}\varphi(\eta, \epsilon)] = \nu^{rp}\Psi(\eta, \nu) - \sum_{j=0}^{r-1} \nu^{p(r-j)-2} D_\epsilon^{jp}\varphi(\eta, 0),\ 0 < p \leqslant 1, \tag{1}$$

where $\eta = (\eta_1, \eta_2, \cdots, \eta_p) \in \mathbb{R}^p$ and $p \in \mathbb{N}$ and $D_\epsilon^{rp} = D_\epsilon^p.D_\epsilon^p.\cdots.D_\epsilon^p(r - times)$

Proof. Let's use induction to verify equation (1). By setting $r = 1$ in equation (1), we obtain:

$$A[D_\epsilon^{2p}\varphi(\eta, \epsilon)] = \nu^{2p}\Psi(\eta, \nu) - \nu^{2p-2}\varphi(\eta, 0) - \nu^{p-2}D_\epsilon^p\varphi(\eta, 0).$$

Part (4) of lemma 2.1 supports the validity of equation (1) for $r = 1$. Putting $r = 2$ in equation (1) gives us

$$A[D_r^{2p}\varphi(\eta, \epsilon)] = \nu^{2p}\Psi(\eta, \nu) - \nu^{2p-2}\varphi(\eta, 0) - \nu^{p-2}D_\epsilon^p\varphi(\eta, 0). \tag{2}$$

Considering L.H.S. of equation (2), we get

$$L.H.S = A[D_\epsilon^{2p}\varphi(\eta, \epsilon)]. \tag{3}$$

The equation (3) may be expressed in a particular manner as

$$L.H.S = A[D_\epsilon^{p}\varphi(\eta, \epsilon)]. \tag{4}$$

Let

$$z(\eta, \epsilon) = D_\epsilon^p\varphi(\eta, \epsilon). \tag{5}$$

As a result, equation (4) becomes

$$L.H.S = A[D_\epsilon^p z(\eta, \epsilon)]. \tag{6}$$

By using the Caputo type fractional derivative.

$$L.H.S = A[J^{1-p}z'(\eta, \epsilon)]. \tag{7}$$

The Aboodh transform's R-L fractional integral formula may be found in equation (7), which gives

$$L.H.S = \frac{A[z'(\eta, \epsilon)]}{\nu^{1-p}}. \tag{8}$$

Through the use of the Aboodh transform's differential property, equation (8) is converted as:

$$L.H.S = \nu^p Z(\eta, \nu) - \frac{z(\eta, 0)}{\nu^{2-p}}, \tag{9}$$

From equation (5), we get

$$Z(\eta, \nu) = \nu^p\Psi(\eta, \nu) - \frac{\varphi(\eta, 0)}{\nu^{2-p}},$$

where $A[z(\eta, \epsilon)] = Z(\eta, \nu)$. As a result, equation (9) is transformed into

$$L.H.S = \nu^{2p}\Psi(\eta, \nu) - \frac{\varphi(\eta, 0)}{\nu^{2-2p}} - \frac{D_\epsilon^p\varphi(\eta, 0)}{\nu^{2-p}}, \tag{10}$$

equation (1) and equation (10) are compatible. Let us now suppose that for $r = K$, equation (1) holds. Put $r = K$ in equation (1) as a result:

$$A[D_\epsilon^{Kp}\varphi(\eta, \epsilon)] = \nu^{Kp}\Psi(\eta, \nu) - \sum_{j=0}^{K-1} \nu^{p(K-j)-2} D_\epsilon^{jp} D_\epsilon^{jp}\varphi(\eta, 0),\ 0 < p \leqslant 1. \tag{11}$$

Here, we'll show that equation (1) is true for $r = K + 1$. To derive equation (1) we write

$$A[D_\epsilon^{(K+1)p}\varphi(\eta, \epsilon)] = \nu^{(K+1)p}\Psi(\eta, \nu) - \sum_{j=0}^{K} \nu^{p((K+1)-j)-2} D_\epsilon^{jp}\varphi(\eta, 0). \tag{12}$$

Using equation (12) left-hand side, we get

$$L.H.S = A[D_{\epsilon}^{Kp}(D_{\epsilon}^{Kp})]. \tag{13}$$

Consider

$$D_{\epsilon}^{Kp} = g(\eta, \epsilon).$$

equation (13) gives us

$$L.H.S = A[D_{\epsilon}^{p} g(\eta, \epsilon)]. \tag{14}$$

The following is an expression for equation (14) using the R-L integral formula and the Caputo fractional derivative:

$$L.H.S = \nu^{p} A[D_{\epsilon}^{Kp} \varphi(\eta, \epsilon)] - \frac{g(\eta, 0)}{\nu^{2-p}}. \tag{15}$$

By ulatizing equation (11), equation (15) is transformed into

$$L.H.S = \nu^{rp} \Psi(\eta, \nu) - \sum_{j=0}^{r-1} \nu^{p(r-j)-2} D_{\epsilon}^{jp} \varphi(\eta, 0), \tag{16}$$

We get the following result by using equation (16).

$$L.H.S = A[D_{\epsilon}^{rp} \varphi(\eta, 0)].$$

It implies that the formula equation (1) hold for $r = K + 1$. Consequently, we used the mathematical induction approach to show that the formula equation (1) holds true for all positive numbers. In the following lemma, we provide a revised version of the multiple fractional Taylor's formula that will be useful for the ARPSM. □

Lemma 2.3. *Suppose that $\varphi(\eta, \epsilon)$ is an exponentially ordered function. Then, $A[\varphi(\eta, \epsilon)] = \Psi(\eta, \nu)$ represents the Aboodh transform of $\varphi(\eta, \epsilon)$ as a multiple fractional Taylor's series:*

$$\Psi(\eta, \nu) = \sum_{r=0}^{\infty} \frac{\hbar_r(\eta)}{\nu^{rp+2}}, \nu > 0, \tag{17}$$

where, $\eta = (s_1, \eta_2, \cdots, \eta_p) \in \mathbb{R}^p$, $p \in \mathbb{N}$.

Proof. When fractional order analysis of Taylor's series is performed, we get

$$\varphi(\eta, \epsilon) = \hbar_0(\eta) + \hbar_1(\eta) \frac{\epsilon^p}{\Gamma[p+1]} ++ \hbar_2(\eta) \frac{\epsilon^{2p}}{\Gamma[2p+1]} + \cdots. \tag{18}$$

By using the Aboodh transform on 18, we get the equality that follows:

$$A[\varphi(\eta, \epsilon)] = A[\hbar_0(\eta)] + A\left[\hbar_1(\eta) \frac{\epsilon^p}{\Gamma[p+1]}\right] + A\left[\hbar_1(\eta) \frac{\epsilon^{2p}}{\Gamma[2p+1]}\right] + \cdots$$

Thus, by using the Aboodh transform's properties, we obtain

$$A[\varphi(\eta, \epsilon)] = \hbar_0(\eta) \frac{1}{\nu^2} + \hbar_1(\eta) \frac{\Gamma[p+1]}{\Gamma[p+1]} \frac{1}{\nu^{p+2}} + \hbar_2(\eta) \frac{\Gamma[2p+1]}{\Gamma[2p+1]} \frac{1}{\nu^{2p+2}} \cdots$$

As a result, 17, a new Taylor's series in the Aboodh transform, is obtained. □

Lemma 2.4. *Suppose that the MFPS representation of the function $A[\varphi(\eta, \epsilon)] = \Psi(\eta, \nu)$ exists in the new form of Taylor's series 17.*

$$\hbar_0(\eta) = \lim_{\nu \to \infty} \nu^2 \Psi(\eta, \nu) = \varphi(\eta, 0). \tag{19}$$

Proof. This previous is based on the new form of Taylor's series.

$$\hbar_0(\eta) = \nu^2 \Psi(\eta, \nu) - \frac{\hbar_1(\eta)}{\nu^p} - \frac{\hbar_2(\eta)}{\nu^{2p}} - \cdots \tag{20}$$

The necessary result, denoted by 19, is obtained by applying $\lim_{\nu \to \infty}$ to equation (20) and performing a short computation. □

Theorem 2.5. *Let $A[\varphi(\eta, \epsilon)] = \Psi(\eta, \nu)$ be the function for which the MFPS representation is provided by*

$$\Psi(\eta, \nu) = \sum_{0}^{\infty} \frac{\hbar_r(\eta)}{\nu^{rp+2}}, \nu > 0,$$

where $\eta = (\eta_1, \eta_2, \cdots, \eta_p) \in \mathbb{R}^p$ *and* $p \in \mathbb{N}$. *Then we have*

$$\hbar_r(\eta) = D_r^{rp}\varphi(\eta, 0),$$

where, $D_\epsilon^{rp} = D_\epsilon^p.D_\epsilon^p.\cdots.D_\epsilon^p(r - times)$.

Proof. From the modified Taylor's series format, we have

$$\hbar_1(\eta) = \nu^{p+2}\Psi(\eta, \nu) - \nu^p\hbar_0(\eta) - \frac{\hbar_2(\eta)}{\nu^p} - \frac{\hbar_3(\eta)}{\nu^{2p}} - \cdots \tag{21}$$

After solving equation (21) with $\lim_{\nu\to\infty}$, we get

$$\hbar_1(\eta) = \lim_{\nu\to\infty}(\nu^{p+2}\Psi(\eta, \nu) - \nu^p\hbar_0(\eta)) - \lim_{\nu\to\infty}\frac{\hbar_2(\eta)}{\nu^p} - \lim_{\nu\to\infty}\frac{\hbar_3(\eta)}{\nu^{2p}} - \cdots$$

After taking the limit, we have the following equality:

$$\hbar_1(\eta) = \lim_{\nu\to\infty}(\nu^{p+2}\Psi(\eta, \nu) - \nu^p\hbar_0(\eta)). \tag{22}$$

Using lemma 2.2 along with equation (22), it becomes

$$\hbar_1(\eta) = \lim_{\nu\to\infty}(\nu^2 A[D_\epsilon^p\varphi(\eta, \epsilon)](\nu)). \tag{23}$$

Moreover, using lemma 2.3 along with equation (23), it becomes

$$\hbar_1(\eta) = D_\epsilon^p\varphi(\eta, 0).$$

Using $\nu \to \infty$ and the modified form of Taylor's series, we get

$$\hbar_2(\eta) = \nu^{2p+2}\Psi(\eta, \nu) - \nu^{2p}\hbar_0(\eta) - \nu^p\hbar_1(\eta) - \frac{\hbar_3(\eta)}{\nu^p} - \cdots$$

Lemma 2.3 gives us

$$\hbar_2(\eta) = \lim_{\nu\to\infty}\nu^2(\nu^{2p}\Psi(\eta, \nu) - \nu^{2p-2}\hbar_0(\eta) - \nu^{p-2}\hbar_1(\eta)). \tag{24}$$

Using lemmas 2.2 and 2.4 again, equation (24) becomes

$$\hbar_2(\eta) = D_\epsilon^{2p}\varphi(\eta, 0).$$

Using the new Taylor's series and the same procedure, we have

$$\hbar_3(\eta) = \lim_{\nu\to\infty}\nu^2(A[D_\epsilon^{2p}\varphi(\eta, p)](\nu)).$$

When lemma 2.4 is applied, the final equation is produced.

$$\hbar_3(\eta) = D_\epsilon^{3p}\varphi(\eta, 0).$$

In general we get

$$\hbar_r(\eta) = D_\epsilon^{rp}\varphi(\eta, 0).$$

Thus, the proof is ended. □

In the following theorem, we demonstrate the necessary and sufficient conditions for the convergence of the modified Taylor formula.

Theorem 2.6. *Lemma 2.3 presents a revised Multiple Fractional Taylor's formula represented as* $A[\varphi(\eta, \epsilon)] = \Psi(\eta, \nu)$. *The remainder* $R_K(\eta, \nu)$ *of the new multiple fractional Taylor's formula for* $(0 < \nu \leqslant s)$ *with* $0 < p \leqslant 1)$ *corresponds to the following inequality if* $|\nu^a A[D_\epsilon^{(K+1)p}\varphi(\eta, \epsilon)]| \leqslant T$.

$$|R_K(\eta, \nu)| \leqslant \frac{T}{\nu^{(K=1)p+2}}, 0 < \nu \leqslant s.$$

Proof. We make the following assumption to start the proof, $A[D_\epsilon^{rp}\varphi(\eta, \epsilon)](\nu)$ is defined on $0 < \nu \leqslant s$ for $r = 0, 1, 2, \cdots, K + 1$. As given, assume that $|\nu^2 A[D_{\epsilon^{K+1}}\varphi(\eta, tau)]| \leqslant T$, *on* $0 < \nu \leqslant s$. Consider the relationship that follows from the new form of Taylor's series:

$$R_K(\eta, \nu) = \Psi(\eta, \nu) - \sum_{r=0}^{K} \frac{\hbar_r(\eta)}{\nu^{rp+2}}. \tag{25}$$

By applying theorem 2.5, equation (25) becomes

$$R_K(\eta, \nu) = \Psi(\eta, \nu) - \sum_{r=0}^{K} \frac{D_\epsilon^{rp}\varphi(\eta, 0)}{\nu^{rp+2}}. \tag{26}$$

Multiply both sides of equation (26) by $\nu^{(K+1)a\ +\ 2}$. As we have

$$\nu^{(K+1)p+2}R_K(\eta, \nu) = \nu^2(\nu^{(K+1)p}\Psi(\eta, \nu) - \sum_{r=0}^{K} \nu^{(K+1-r)p-2}D_\epsilon^{rp}\varphi(\eta, 0)). \tag{27}$$

Applying lemma 2.2 to equation (27) yields

$$\nu^{(K+1)p+2}R_K(\eta, \nu) = \nu^2 A[D_\epsilon^{(K+1)p}\varphi(\eta, \epsilon)]. \tag{28}$$

When we apply the absolute sign to equation (28), we get

$$|\nu^{(K+1)p+2}R_K(\eta, \nu)| = |\nu^2 A[D_\epsilon^{(K+1)p}\varphi(\eta, \epsilon)]|. \tag{29}$$

The following is the result we get by applying the condition given in equation (29), and hence

$$\frac{-T}{\nu^{(K+1)p+2}} \leqslant R_K(\eta, \nu) \leqslant \frac{T}{\nu^{(K+1)p+2}}. \tag{30}$$

Equation (30) provides the necessary outcome.

$$|R_K(\eta, \nu)| \leqslant \frac{T}{\nu^{(K+1)p+2}}.$$

This leads to the establishment of the new series convergence condition. □

3. Road map for the suggested techniques

3.1. The ARPSM method for solving time-fractional PDEs with arbitrary coefficients

We provide the guiding principles of the ARPSM for solving our generic model.

Step 1: Rewrite the equation in general. As we have

$$D_\epsilon^{qp}\varphi(\eta, \epsilon) + \vartheta(\eta)N(\varphi) - \zeta(\eta, \varphi) = 0, \tag{31}$$

Step 2: Aboodh transformation applied to both sides of equation (31) gives

$$A[D_\epsilon^{qp}\varphi(\eta, \epsilon) + \vartheta(\eta)N(\varphi) - \zeta(\eta, \varphi)] = 0, \tag{32}$$

Using lemma 2.2, we transform equation (32).

$$\Psi(\eta, s) = \sum_{j=0}^{q-1} \frac{D_\epsilon^{j}\varphi(\eta, 0)}{s^{qp+2}} - \frac{\vartheta(\eta)Y(s)}{s^{qp}} + \frac{F(\eta, s)}{s^{qp}}, \tag{33}$$

where, $A[\zeta(\eta, \varphi)] = F(\eta, s)$, $A[N(\varphi)] = Y(s)$.

Step 3: To solve equation (33), take into account the following form:

$$\Psi(\eta, s) = \sum_{r=0}^{\infty} \frac{\hbar_r(\eta)}{s^{rp+2}},\ s > 0,$$

Step 4: Follow the steps given below:

$$\hbar_0(\eta) = \lim_{s\to\infty} s^2\Psi(\eta, s) = \varphi(\eta, 0),$$

and we get the following by using theorem 2.6.

$$\begin{aligned}
\hbar_1(\eta) &= D_\epsilon^{p}\varphi(\eta, 0),\\
\hbar_2(\eta) &= D_\epsilon^{2p}\varphi(\eta, 0),\\
&\vdots\\
\hbar_w(\eta) &= D_\epsilon^{wp}\varphi(\eta, 0),
\end{aligned}$$

Step 5: Obtain $\Psi(\eta, s)$ as the K^{th}-truncated series as follows:

$$\Psi_K(\eta, s) = \sum_{r=0}^{K} \frac{\hbar_r(\eta)}{s^{rp+2}},\ s > 0,$$

$$\Psi_K(\eta, s) = \frac{\hbar_0(\eta)}{s^2} + \frac{\hbar_1(\eta)}{s^{p+2}} + \cdots + \frac{\hbar_w(\eta)}{s^{wp+2}} + \sum_{r=w+1}^{K} \frac{\hbar_r(\eta)}{s^{rp+2}},$$

Step 6: The Aboodh residual function (ARF) of equation (33) to be examined independently of the K^{th}-truncated Aboodh residual function in order to get

$$ARes(\eta, s) = \Psi(\eta, s) - \sum_{j=0}^{q-1} \frac{D_\epsilon^j \varphi(\eta, 0)}{s^{jp+2}} + \frac{\vartheta(\eta) Y(s)}{s^{jp}} - \frac{F(\eta, s)}{s^{jp}},$$

and

$$ARes_K(\eta, s) = \Psi_K(\eta, s) - \sum_{j=0}^{q-1} \frac{D_\epsilon^j \varphi(\eta, 0)}{s^{jp+2}} + \frac{\vartheta(\eta) Y(s)}{s^{jp}} - \frac{F(\eta, s)}{s^{jp}}. \tag{34}$$

Step 7: In equation (34), substitute the expansion form of $\Psi_K(\eta, s)$.

$$ARes_K(\eta, s) = \left(\frac{\hbar_0(\eta)}{s^2} + \frac{\hbar_1(\eta)}{s^{p+2}} + \cdots + \frac{\hbar_w(\eta)}{s^{wp+2}} + \sum_{r=w+1}^{K} \frac{\hbar_r(\eta)}{s^{rp+2}} \right) - \sum_{j=0}^{q-1} \frac{D_\epsilon^j \varphi(\eta, 0)}{s^{jp+2}} + \frac{\vartheta(\eta) Y(s)}{s^{jp}} - \frac{F(\eta, s)}{s^{jp}}. \tag{35}$$

Step 8: Multiply both sides of equation (35) by s^{Kp+2}

$$s^{Kp+2} ARes_K(\eta, s) = s^{Kp+2} \left(\frac{\hbar_0(\eta)}{s^2} + \frac{\hbar_1(\eta)}{s^{p+2}} + \cdots + \frac{\hbar_w(\eta)}{s^{wp+2}} + \sum_{r=w+1}^{K} \frac{\hbar_r(\eta)}{s^{rp+2}} - \sum_{j=0}^{q-1} \frac{D_\epsilon^j \varphi(\eta, 0)}{s^{jp+2}} + \frac{\vartheta(\eta) Y(s)}{s^{jp}} - \frac{F(\eta, s)}{s^{jp}} \right). \tag{36}$$

Step 9: Taking $\lim_{s\to\infty}$ on both sides of equation (36):

$$\lim_{s\to\infty} s^{Kp+2} ARes_K(\eta, s) = \lim_{s\to\infty} s^{Kp+2} \left(\frac{\hbar_0(\eta)}{s^2} + \frac{\hbar_1(\eta)}{s^{p+2}} + \cdots + \frac{\hbar_w(\eta)}{s^{wp+2}} + \sum_{r=w+1}^{K} \frac{\hbar_r(\eta)}{s^{rp+2}} - \sum_{j=0}^{q-1} \frac{D_\epsilon^j \varphi(\eta, 0)}{s^{jp+2}} + \frac{\vartheta(\eta) Y(s)}{s^{jp}} - \frac{F(\eta, s)}{s^{jp}} \right).$$

Step 10: We need to solve the following equation for $\hbar_K(\eta)$.

$$\lim_{s\to\infty} (s^{Kp+2} ARes_K(\eta, s)) = 0,$$

where $K = w+1, w+2, \cdots$.

Step 11: The K-approximate solution of equation (33) may be found by substituting the obtained values of $\hbar_K(\eta)$ into the K-truncated series of $\Psi(\eta, s)$.

Step 12:The K-approximate solution $\varphi_K(\eta, \epsilon)$ may be obtained by using the inverse Aboodh transform on $\Psi_K(\eta, s)$.

3.2. Problem

Consider the fractional DSW system as:

$$D_\epsilon^p \varphi_a(\eta, \epsilon) + 3\varphi_b(\eta, \epsilon) \frac{\partial \varphi_b(\eta, \epsilon)}{\partial \eta} = 0, \tag{37}$$

$$D_\epsilon^p \varphi_b(\eta, \epsilon) + 2\frac{\partial^3 \varphi_b(\eta, \epsilon)}{\partial \eta^3} + 2\varphi_a(\eta, \epsilon) \frac{\partial \varphi_b(\eta, \epsilon)}{\partial \eta} + \varphi_b(\eta, \epsilon) \frac{\partial \varphi_a(\eta, \epsilon)}{\partial \eta} = 0, \quad \text{where} \quad 0 < p \leqslant 1 \tag{38}$$

Subjected to the following IC's:

$$\varphi_a(\eta, 0) = \frac{3c}{2} \operatorname{sech}^2\left(\sqrt{\frac{c}{2}} \eta \right). \tag{39}$$

$$\varphi_b(\eta, 0) = c \operatorname{sech}\left(\sqrt{\frac{c}{2}} \eta \right). \tag{40}$$

Applying AT to Eq (37) and (38) and making use of equation (39) and (40) respectively, we get

$$\varphi_a(\eta,\,\epsilon) - \frac{\frac{3c}{2}\,\mathrm{sech}^2\left(\sqrt{\frac{c}{2}}\eta\right)}{s^2} + \frac{3}{s^p}\mathcal{A}_\epsilon\left[\mathcal{A}_\epsilon^{-1}\varphi_b(\eta,\,\epsilon) \times \frac{\partial\mathcal{A}_\epsilon^{-1}\varphi_b(\eta,\,\epsilon)}{\partial\eta}\right] = 0, \tag{41}$$

$$\varphi_b(\eta,\,\epsilon) - \frac{c\,\mathrm{sech}\left(\sqrt{\frac{c}{2}}\eta\right)}{s^2} + \frac{2}{s^p}\left[\frac{\partial^3\varphi_b(\eta,\,\epsilon)}{\partial\eta^3}\right] + \frac{2}{s^p}\mathcal{A}_\epsilon\left[\mathcal{A}_\epsilon^{-1}\varphi_a(\eta,\,\epsilon) \times \frac{\partial\mathcal{A}_\epsilon^{-1}\varphi_b(\eta,\,\epsilon)}{\partial\eta}\right] + \frac{1}{s^p}\mathcal{A}_\epsilon\left[\mathcal{A}_\epsilon^{-1}\varphi_b(\eta,\,\epsilon) \times \frac{\partial\mathcal{A}_\epsilon^{-1}\varphi_a(\eta,\,\epsilon)}{\partial\eta}\right] = 0, \tag{42}$$

and so the k^{th}-truncated term series are

$$\varphi_a(\eta,\,s) = \frac{\frac{3c}{2}\,\mathrm{sech}^2\left(\sqrt{\frac{c}{2}}\eta\right)}{s^2} + \sum_{r=1}^{k}\frac{f_r(\eta,\,s)}{s^{rp+1}},\quad r = 1,\,2,\,3,\,4\,\cdots. \tag{43}$$

$$\varphi_b(\eta,\,s) = \frac{c\,\mathrm{sech}\left(\sqrt{\frac{c}{2}}\eta\right)}{s^2} + \sum_{r=1}^{k}\frac{g_r(\eta,\,s)}{s^{rp+1}},\quad r = 1,\,2,\,3,\,4\,\cdots. \tag{44}$$

Aboodh residual functions (ARFs) are

$$\mathcal{A}_\epsilon\,Res(\eta,\,s) = \varphi_a(\eta,\,\epsilon) - \frac{\frac{3c}{2}\,\mathrm{sech}^2\left(\sqrt{\frac{c}{2}}\eta\right)}{s^2} + \frac{3}{s^p}\mathcal{A}_\epsilon\left[\mathcal{A}_\epsilon^{-1}\varphi_b(\eta,\,\epsilon) \times \frac{\partial\mathcal{A}_\epsilon^{-1}\varphi_b(\eta,\,\epsilon)}{\partial\eta}\right] = 0 \tag{45}$$

$$\mathcal{A}_\epsilon\,Res(\eta,\,s) = \varphi_b(\eta,\,\epsilon) - \frac{c\,\mathrm{sech}\left(\sqrt{\frac{c}{2}}\eta\right)}{s^2} + \frac{2}{s^p}\left[\frac{\partial^3\varphi_b(\eta,\,\epsilon)}{\partial\eta^3}\right] + \frac{2}{s^p}\mathcal{A}_\epsilon\left[\mathcal{A}_\epsilon^{-1}\varphi_a(\eta,\,\epsilon) \times \frac{\partial\mathcal{A}_\epsilon^{-1}\varphi_b(\eta,\,\epsilon)}{\partial\eta}\right] + \frac{1}{s^p}\mathcal{A}_\epsilon\left[\mathcal{A}_\epsilon^{-1}\varphi_b(\eta,\,\epsilon) \times \frac{\partial\mathcal{A}_\epsilon^{-1}\varphi_a(\eta,\,\epsilon)}{\partial\eta}\right] = 0 \tag{46}$$

and the k^{th}-LRFs as:

$$\mathcal{A}_\epsilon Res_k(\eta,\,s) = \varphi_{ak}(\eta,\,\epsilon) - \frac{\frac{3c}{2}\,\mathrm{sech}^2\left(\sqrt{\frac{c}{2}}\eta\right)}{s^2} + \frac{3}{s^p}\mathcal{A}_\epsilon\left[\mathcal{A}_\epsilon^{-1}\varphi_{bk}(\eta,\,\epsilon) \times \frac{\partial\mathcal{A}_\epsilon^{-1}\varphi_{bk}(\eta,\,\epsilon)}{\partial\eta}\right] = 0 \tag{47}$$

$$\mathcal{A}_\epsilon Res_k(\eta,\,s) = \varphi_{bk}(\eta,\,\epsilon) - \frac{c\,\mathrm{sech}\left(\sqrt{\frac{c}{2}}\eta\right)}{s^2} + \frac{2}{s^p}\left[\frac{\partial^3\varphi_{bk}(\eta,\,\epsilon)}{\partial\eta^3}\right] + \frac{2}{s^p}\mathcal{A}_\epsilon[\mathcal{A}_\epsilon^{-1}\varphi_{ak}(\eta,\,\epsilon) \times \frac{\partial\mathcal{A}_\epsilon^{-1}\varphi_{bk}(\eta,\,\epsilon)}{\partial\eta}] + \frac{1}{s^p}\mathcal{A}_\epsilon\left[\mathcal{A}_\epsilon^{-1}\varphi_{bk}(\eta,\,\epsilon) \times \frac{\partial\mathcal{A}_\epsilon^{-1}\varphi_{ak}(\eta,\,\epsilon)}{\partial\eta}\right] = 0 \tag{48}$$

In order to calculate $f_r(\eta, s)$ and $g_r(\eta, s)$, we multiply the resultant equations by s^{rp+1}, replace the r^{th}-truncated series equation (43) and (44) into the r^{th}-Aboodh residual function equation (47) and (48), and solve the relation $\lim_{s\to\infty}(s^{rp+1}A_\epsilon\,Res_{\varphi,r}(\eta,\,s)) = 0$ iteratively, $r = 1, 2, 3, \cdots$.

Here are the first few of terms:

$$f_1(\eta,\,s) = \frac{3c^{5/2}\tanh\left(\frac{\sqrt{c}\eta}{\sqrt{2}}\right)\mathrm{sech}^2\left(\frac{\sqrt{c}\eta}{\sqrt{2}}\right)}{\sqrt{2}},$$
$$g_1(\eta,\,s) = \frac{c^{5/2}\tanh\left(\frac{\sqrt{c}\eta}{\sqrt{2}}\right)\mathrm{sech}\left(\frac{\sqrt{c}\eta}{\sqrt{2}}\right)}{\sqrt{2}}, \tag{49}$$

$$f_2(\eta,\,s) = \frac{3}{2}c^4(\cosh(\sqrt{2}\,\sqrt{c}\eta) - 2)\,\mathrm{sech}^4\left(\frac{\sqrt{c}\eta}{\sqrt{2}}\right),$$
$$g_2(\eta,\,s) = \frac{1}{4}c^4(\cosh(\sqrt{2}\,\sqrt{c}\eta) - 3)\,\mathrm{sech}^3\left(\frac{\sqrt{c}\eta}{\sqrt{2}}\right). \tag{50}$$

and so on.

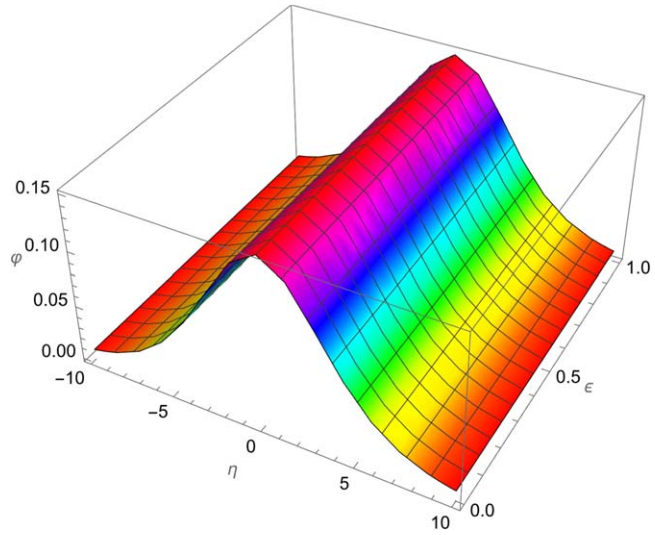

Figure 1. ARPSM solution $\varphi_a(\eta, \epsilon)$ for $p = 1.0$ and $\epsilon = 1.5$.

Putting the values of $f_r(\eta, s)$ and $g_r(\eta, s)$, $r = 1, 2, 3, \cdots$, in equation (43), (44), we get

$$\varphi_a(\eta, s) = \frac{3c^{5/2}\tanh\left(\frac{\sqrt{c}\eta}{\sqrt{2}}\right)\operatorname{sech}^2\left(\frac{\sqrt{c}\eta}{\sqrt{2}}\right)}{\sqrt{2}\,s^{p+1}} + \frac{3c^4(\cosh(\sqrt{2}\sqrt{c}\eta) - 2)\operatorname{sech}^4\left(\frac{\sqrt{c}\eta}{\sqrt{2}}\right)}{2s^{2p+1}} + \frac{(3c)\operatorname{sech}^2\left(\sqrt{\frac{c}{2}}\eta\right)}{2s} + \cdots. \tag{51}$$

$$\varphi_b(\eta, s) = \frac{c^{5/2}\tanh\left(\frac{\sqrt{c}\eta}{\sqrt{2}}\right)\operatorname{sech}\left(\frac{\sqrt{c}\eta}{\sqrt{2}}\right)}{\sqrt{2}\,s^{p+1}} + \frac{c^4(\cosh(\sqrt{2}\sqrt{c}\eta) - 3)\operatorname{sech}^3\left(\frac{\sqrt{c}\eta}{\sqrt{2}}\right)}{4s^{2p+1}} + \frac{c\operatorname{sech}\left(\sqrt{\frac{c}{2}}\eta\right)}{s} + \cdots. \tag{52}$$

Using Aboodh inverse transform,we get

$$\varphi_a(\eta, s) = \frac{3c^{5/2}\epsilon^p\tanh\left(\frac{\sqrt{c}\eta}{\sqrt{2}}\right)\operatorname{sech}^2\left(\frac{\sqrt{c}\eta}{\sqrt{2}}\right)}{\sqrt{2}\,\Gamma(p+1)} - \frac{3c^4\epsilon^{2p}\operatorname{sech}^4\left(\frac{\sqrt{c}\eta}{\sqrt{2}}\right)}{\Gamma(2p+1)} + \frac{3c^4\epsilon^{2p}\cosh(\sqrt{2}\sqrt{c}\eta)\operatorname{sech}^4\left(\frac{\sqrt{c}\eta}{\sqrt{2}}\right)}{2\Gamma(2p+1)} + \frac{3}{2}c\operatorname{sech}^2\left(\frac{\sqrt{c}\eta}{\sqrt{2}}\right) + \cdots. \tag{53}$$

$$\varphi_b(\eta, s) = \frac{c^{5/2}\epsilon^p\tanh\left(\frac{\sqrt{c}\eta}{\sqrt{2}}\right)\operatorname{sech}\left(\frac{\sqrt{c}\eta}{\sqrt{2}}\right)}{\sqrt{2}\,\Gamma(p+1)} - \frac{3c^4\epsilon^{2p}\operatorname{sech}^3\left(\frac{\sqrt{c}\eta}{\sqrt{2}}\right)}{4\Gamma(2p+1)} + \frac{c^4\epsilon^{2p}\cosh(\sqrt{2}\sqrt{c}\eta)\operatorname{sech}^3\left(\frac{\sqrt{c}\eta}{\sqrt{2}}\right)}{4\Gamma(2p+1)} + c\operatorname{sech}\left(\frac{\sqrt{c}\eta}{\sqrt{2}}\right) + \cdots. \tag{54}$$

Figure 1 portrays the Aboodh Residual Power Series Method (ARPSM) solution, $\varphi_a(\eta, \epsilon)$, for a specific set of parameters ($p = 1.0$ and $\epsilon = 1.5$). Meanwhile, figure 2 exhibits the exact solution, $\varphi_a(\eta, \epsilon)$, specifically at $\epsilon = 1.5$. Comparing these figures reveals the similarity or divergence between the ARPSM-derived solution and the exact solution at the given parameter values. Figure 3 presents a comparative analysis between the exact solution $\varphi_a(\eta, \epsilon)$ (at $\epsilon = 1.5$) and the ARPSM solution for the same parameter values. This direct comparison provides insights into the accuracy and reliability of the ARPSM method in approximating the exact solution under the specified conditions. Similar to figures 1 and 2, figure 4 displays the ARPSM solution $\varphi_b(\eta, \epsilon)$ for $p = 1.0$ and $\epsilon = 1.5$, while figure 5 showcases the exact solution $\varphi_b(\eta, \epsilon)$ at $\epsilon = 1.5$. These graphs allow for an examination of the ARPSM-derived solution against the exact solution for a different scenario or variable in the system. Figure 6 enables a direct comparison between the exact solution $\varphi_b(\eta, \epsilon)$ (at $\epsilon = 1.5$) and the ARPSM solution $\varphi_b(\eta, \epsilon)$ for the given parameter values. This comparison aids in evaluating the accuracy and reliability of the ARPSM method in approximating the exact solution under these specific conditions. Table 1 presents a comparison of different fractional orders of the ARPSM solution $\varphi_a(\eta, \epsilon)$ for $\epsilon = 1.5$ and $c = 0.1$. This tabular representation

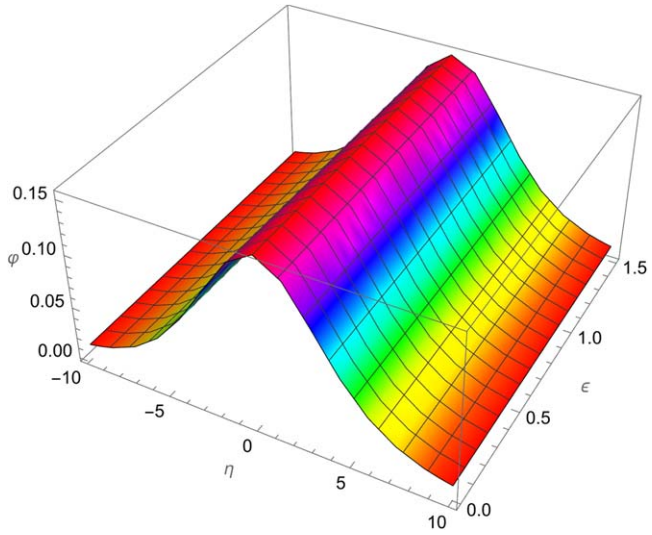

Figure 2. Exact solution $\varphi_a(\eta, \epsilon)$ at $\epsilon = 1.5$.

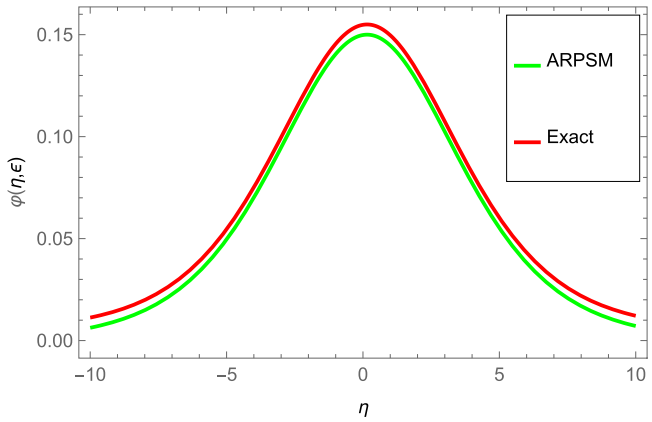

Figure 3. Comparison of exact and ARPSM solution $\varphi_a(\eta, \epsilon)$ at $\epsilon = 1.5$.

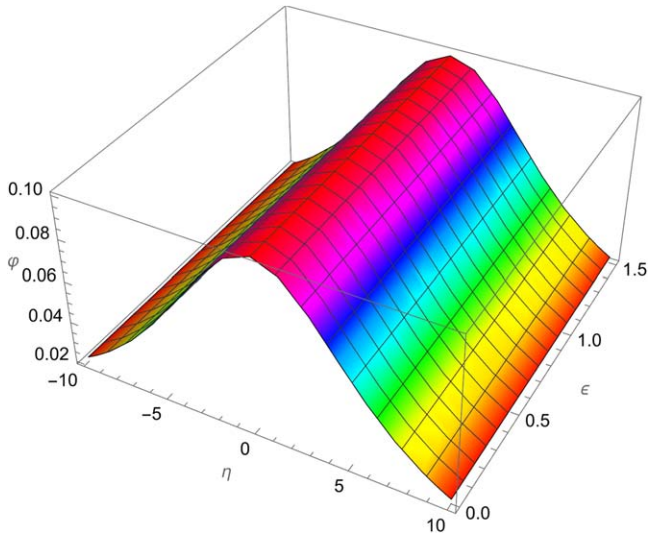

Figure 4. ARPSM solution $\varphi_b(\eta, \epsilon)$ for $p = 1.0$ and $\epsilon = 1.5$.

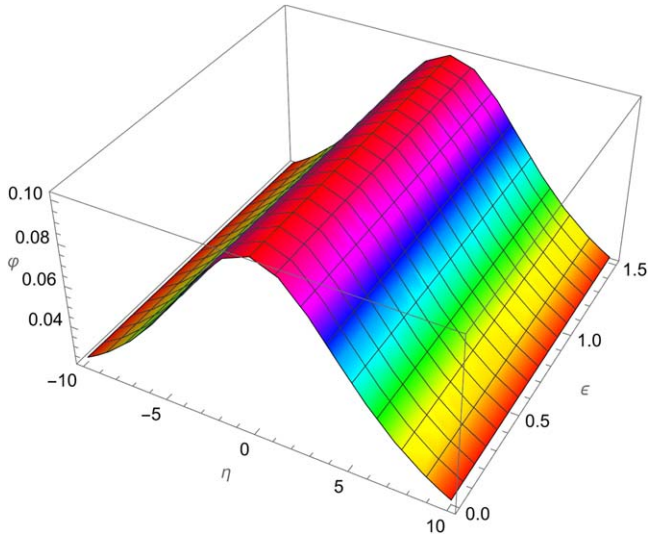

Figure 5. Exact solution $\varphi_b(\eta, \epsilon)$ at $\epsilon = 1.5$.

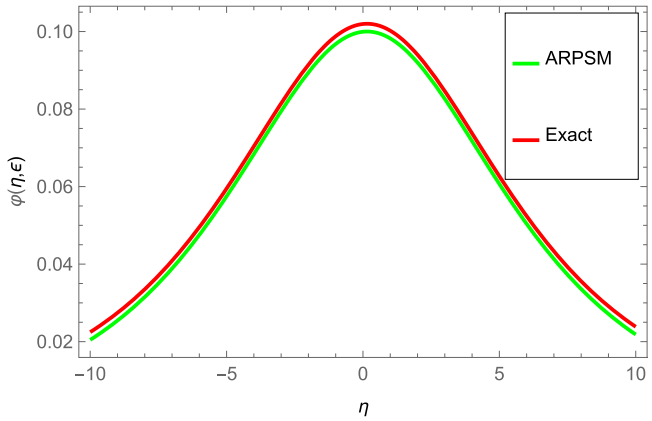

Figure 6. Comparison of exact and ARPSM solution $\varphi_b(\eta, \epsilon)$ at $\epsilon = 1.5$.

Table 1. The comparison of different fractional order of ARPSM solution $\varphi_a(\eta, \epsilon)$ for $\epsilon = 1.5$ and $c = 0.1$.

η	$ARPSM_{P=0.6}$	$ARPSM_{p=0.8}$	$ARPSM_{P=1.0}$	*Exact*	$Error_{p=0.7}$	$Error_{p=0.8}$	$Error_{p=1.0}$
0.	0.149 779	0.149 799	0.149 831	0.149 831	0.000 052 837 4	0.000 032 107 9	1.264818×10^{-7}
0.1	0.149 918	0.149 947	0.149 981	0.149 981	0.000 063 274	0.000 033 946	2.107553×10^{-7}
0.2	0.149 908	0.149 946	0.149 982	0.149 981	0.000 073 459 3	0.000 035 649 8	5.462043×10^{-7}
0.3	0.149 748	0.149 794	0.149 832	0.149 831	0.000 083 355 4	0.000 037 214 6	8.770298×10^{-7}
0.4	0.149 439	0.149 494	0.149 533	0.149 532	0.000 092 927 4	0.000 038 637 4	1.200463×10^{-6}
0.5	0.148 983	0.149 045	0.149 087	0.149 085	0.000 102 143	0.000 039 915 8	1.513842×10^{-6}
0.6	0.148 38	0.148 45	0.148 493	0.148 491	0.000 110 971	0.000 041 048 9	1.814650×10^{-6}
0.7	0.147 635	0.147 712	0.147 756	0.147 754	0.000 119 387	0.000 042 036 8	2.100546×10^{-6}
0.8	0.146 748	0.146 832	0.146 878	0.146 875	0.000 127 366	0.000 042 880 4	2.369398×10^{-6}
0.9	0.145 724	0.145 816	0.145 862	0.145 859	0.000 134 889	0.000 043 581 9	2.619308×10^{-6}
1.	0.144 567	0.144 665	0.144 712	0.144 709	0.000 141 938	0.000 044 144 1	2.848634×10^{-6}

offers a systematic analysis of the ARPSM-derived solutions under various fractional orders, enabling a quantitative assessment of their accuracy and convergence. Similar to table 1, table 2 provides a comparative analysis of different fractional orders of the ARPSM solution $\varphi_b(\eta, \epsilon)$ for $\epsilon = 1.5$ and $c = 0.1$. This table allows for a detailed examination of how different fractional orders affect the accuracy and reliability of the ARPSM-derived solutions for the specific scenario.

Table 2. The comparison of different fractional order of ARPSM solution $\varphi_b(\eta, \epsilon)$ for $\epsilon = 1.5$ and $c = 0.1$.

η	$ARPSM_{P=0.6}$	$ARPSM_{p=0.8}$	$ARPSM_{P=1.0}$	*Exact*	$Error_{p=0.7}$	$Error_{p=0.8}$	$Error_{p=1.0}$
0.	0.099 926 2	0.099 933 1	0.099 943 8	0.099 943 8	0.000 017 596 6	0.000 010 686 8	2.635513×10^{-8}
0.1	0.099 972 6	0.099 982 4	0.099 993 8	0.099 993 8	0.000 021 131 8	0.000 011 349 9	4.391807×10^{-8}
0.2	0.099 969 1	0.099 981 8	0.099 993 9	0.099 993 8	0.000 024 614 3	0.000 011 984 7	1.139237×10^{-7}
0.3	0.099 915 7	0.099 931 2	0.099 944	0.099 943 8	0.000 028 036 1	0.000 012 590 3	1.832369×10^{-7}
0.4	0.099 812 6	0.099 830 8	0.099 844 2	0.099 844	0.000 031 389 4	0.000 013 165 5	2.514403×10^{-7}
0.5	0.099 659 9	0.099 680 8	0.099 694 8	0.099 694 5	0.000 034 666 6	0.000 013 709 5	3.181293×10^{-7}
0.6	0.099 458	0.099 481 7	0.099 496 3	0.099 495 9	0.000 037 861	0.000 014 221 6	3.829159×10^{-7}
0.7	0.099 207 5	0.099 233 8	0.099 248 9	0.099 248 5	0.000 040 965 9	0.000 014 701 5	4.454334×10^{-7}
0.8	0.098 909	0.098 937 8	0.098 953 5	0.098 953	0.000 043 975 4	0.000 015 148 6	5.053397×10^{-7}
0.9	0.098 563 2	0.098 594 5	0.098 610 6	0.098 61	0.000 046 884	0.000 015 563	5.623208×10^{-7}
1.	0.098 170 9	0.098 204 6	0.098 221 2	0.098 220 5	0.000 049 686 8	0.000 015 944 5	6.160938×10^{-7}

3.3. Basic idea of the aboodh transform iterative method

Take the fractional partial differential equation in space and time of the form.

$$D_{\epsilon}^{p}\varphi(\eta, \epsilon) = \Phi(\varphi(\eta, \epsilon), D_{\eta}^{\varphi}\varphi(\eta, \epsilon), D_{\eta}^{2\varphi}\varphi(\eta, \epsilon), D_{\eta}^{3\varphi}\varphi(\eta, \epsilon)), 0 < p, \varphi \leqslant 1, \tag{55}$$

with the initial conditions

$$\varphi^{(k)}(\eta, 0) = h_k, k = 0, 1, 2, \cdots, m-1, \tag{56}$$

$\varphi(\eta, \epsilon)$ is the unknown function to be determine and $\Phi(\varphi(\eta, \epsilon), D_{\eta}^{\varphi}\varphi(\eta, \epsilon), D_{\eta}^{2\varphi}\varphi(\eta, \epsilon), D_{\eta}^{3\varphi}\varphi(\eta, \epsilon))$ can be linear or nonlinear operator of $\varphi(\eta, \epsilon)$, $D_{\eta}^{\varphi}\varphi(\eta, \epsilon)$, $D_{\eta}^{2\varphi}\varphi(\eta, \epsilon)$ and $D_{\eta}^{3\varphi}\varphi(\eta, \epsilon)$ For convenience we represent $\varphi(\eta, \epsilon)$ with φ, Thus, we get the following equation by applying the Aboodh transform to both sides of equation (55):

$$A[\varphi(\eta, \epsilon)] = \frac{1}{s^p}\left(\sum_{k=0}^{m-1}\frac{\varphi^{(k)}(\eta, 0)}{s^{2-p+k}} + A[\Phi(\varphi(\eta, \epsilon), D_{\eta}^{\varphi}\varphi(\eta, \epsilon), D_{\eta}^{2\varphi}\varphi(\eta, \epsilon), D_{\eta}^{3\varphi}\varphi(\eta, \epsilon))]\right), \tag{57}$$

Inverse Aboodh transformation yields the following equation:

$$\varphi(\eta, \epsilon) = A^{-1}\left[\frac{1}{s^p}\left(\sum_{k=0}^{m-1}\frac{\varphi^{(k)}(\eta, 0)}{s^{2-p+k}} + A[\Phi(\varphi(\eta, \epsilon), D_{\eta}^{\varphi}\varphi(\eta, \epsilon), D_{\eta}^{2\varphi}\varphi(\eta, \epsilon), D_{\eta}^{3\varphi}\varphi(\eta, \epsilon))]\right)\right]. \tag{58}$$

An infinite series represents the solution obtained by the Aboodh transform iterative approach.

$$\varphi(\eta, \epsilon) = \sum_{i=0}^{\infty}\varphi_i. \tag{59}$$

As $\Phi(\varphi, D_{\eta}^{\varphi}\varphi, D_{\eta}^{2\varphi}\varphi, D_{\eta}^{3\varphi}\varphi)$ is an operator that can be either linear or nonlinear and is decomposable as follows:

$$\begin{aligned}\Phi(\varphi, D_{\eta}^{\varphi}\varphi, D_{\eta}^{2\varphi}\varphi, D_{\eta}^{3\varphi}\varphi) &= \Phi(\varphi_0, D_{\eta}^{\varphi}\varphi_0, D_{\eta}^{2\varphi}\varphi_0, D_{\eta}^{3\varphi}\varphi_0)\\ &+\sum_{i=0}^{\infty}\left(\Phi\left(\sum_{k=0}^{i}(\varphi_k, D_{\eta}^{\varphi}\varphi_k, D_{\eta}^{2\varphi}\varphi_k, D_{\eta}^{3\varphi}\varphi_k)\right) - \Phi\left(\sum_{k=1}^{i-1}(\varphi_k, D_{\eta}^{\varphi}\varphi_k, D_{\eta}^{2\varphi}\varphi_k, D_{\eta}^{3\varphi}\varphi_k)\right)\right).\end{aligned} \tag{60}$$

The following equation is obtained by substituting equations (60) and (59) into equation (58):

$$\begin{aligned}\sum_{i=0}^{\infty}\varphi_i(\eta, \epsilon) &= A^{-1}\left[\frac{1}{s^p}\left(\sum_{k=0}^{m-1}\frac{\varphi^{(k)}(\eta, 0)}{s^{2-p+k}} + A[\Phi(\varphi_0, D_{\eta}^{\varphi}\varphi_0, D_{\eta}^{2\varphi}\varphi_0, D_{\eta}^{3\varphi}\varphi_0)]\right)\right]\\ &+A^{-1}\left[\frac{1}{s^p}\left(A\left[\sum_{i=0}^{\infty}\left(\Phi\sum_{k=0}^{i}(\varphi_k, D_{\eta}^{\varphi}\varphi_k, D_{\eta}^{2\varphi}\varphi_k, D_{\eta}^{3\varphi}\varphi_k)\right)\right]\right)\right]\\ &-A^{-1}\left[\frac{1}{s^p}\left(A\left[\left(\Phi\sum_{k=1}^{i-1}(\varphi_k, D_{\eta}^{\varphi}\varphi_k, D_{\eta}^{2\varphi}\varphi_k, D_{\eta}^{3\varphi}\varphi_k)\right)\right]\right)\right]\end{aligned} \tag{61}$$

$$\varphi_0(\eta,\,\epsilon) = A^{-1}\left[\frac{1}{s^p}\left(\sum_{k=0}^{m-1}\frac{\varphi^{(k)}(\eta,\,0)}{s^{2-p+k}}\right)\right],$$

$$\varphi_1(\eta,\,\epsilon) = A^{-1}\left[\frac{1}{s^p}(A[\Phi(\varphi_0,\,D_\eta^{\varphi}\varphi_0,\,D_\eta^{2\varphi}\varphi_0,\,D_\eta^{3\varphi}\varphi_0)])\right],$$

$$\vdots$$

$$\varphi_{m+1}(\eta,\,\epsilon) = A^{-1}\left[\frac{1}{s^p}\left(A\left[\sum_{i=0}^{\infty}\left(\Phi\sum_{k=0}^{i}(\varphi_k,\,D_\eta^{\varphi}\varphi_k,\,D_\eta^{2\varphi}\varphi_k,\,D_\eta^{3\varphi}\varphi_k)\right)\right]\right)\right]$$

$$-A^{-1}\left[\frac{1}{s^p}\left(A\left[\left(\Phi\sum_{k=1}^{i-1}(\varphi_k,\,D_\eta^{\varphi}\varphi_k,\,D_\eta^{2\varphi}\varphi_k,\,D_\eta^{3\varphi}\varphi_k)\right)\right]\right)\right],\ m = 1,\,2,\cdots. \tag{62}$$

Equation (55) yields the following analytically approximate solution for the m-term:

$$\varphi(\eta,\,\epsilon) = \sum_{i=0}^{m-1}\varphi_i. \tag{63}$$

3.3.1. Problem with NITM

$$D_\epsilon^p\varphi_a(\eta,\,\epsilon) = -3\varphi_b(\eta,\,\epsilon)\frac{\partial\varphi_b(\eta,\,\epsilon)}{\partial\eta}, \tag{64}$$

$$D_\epsilon^p\varphi_b(\eta,\,\epsilon) = -2\frac{\partial^3\varphi_b(\eta,\,\epsilon)}{\partial\eta^3} - 2\varphi_a(\eta,\,\epsilon)\frac{\partial\varphi_b(\eta,\,\epsilon)}{\partial\eta} - \varphi_b(\eta,\,\epsilon)\frac{\partial\varphi_a(\eta,\,\epsilon)}{\partial\eta},\ \text{where}\ \ 0 < p \leqslant 1 \tag{65}$$

Subjected to the following IC's:

$$\varphi_a(\eta,\,0) = \frac{3c}{2}\,\mathrm{sech}^2\left(\sqrt{\frac{c}{2}}\,\eta\right). \tag{66}$$

$$\varphi_b(\eta,\,0) = c\ \mathrm{sech}\left(\sqrt{\frac{c}{2}}\,\eta\right). \tag{67}$$

When the Aboodh transform is applied to both sides of equations (64) and (65), the following equations develop:

$$A[D_\epsilon^p\varphi_a(\eta,\,\epsilon)] = \frac{1}{s^p}\left(\sum_{k=0}^{m-1}\frac{\varphi_a^{(k)}(\eta,\,0)}{s^{2-p+k}} + A\left[-3\varphi_b(\eta,\,\epsilon)\frac{\partial\varphi_b(\eta,\,\epsilon)}{\partial\eta}\right]\right) \tag{68}$$

$$A[D_\epsilon^p\varphi_b(\eta,\,\epsilon)] = \frac{1}{s^p}\left(\sum_{k=0}^{m-1}\frac{\varphi_b^{(k)}(\eta,\,0)}{s^{2-p+k}} + A\left[-2\frac{\partial^3\varphi_b(\eta,\,\epsilon)}{\partial\eta^3} - 2\varphi_a(\eta,\,\epsilon)\frac{\partial\varphi_b(\eta,\,\epsilon)}{\partial\eta} - \varphi_b(\eta,\,\epsilon)\frac{\partial\varphi_a(\eta,\,\epsilon)}{\partial\eta}\right]\right) \tag{69}$$

The following equations are obtained by applying the inverse Aboodh transform to equations (68) and 69:

$$\varphi(\eta,\,\epsilon) = A^{-1}\left[\frac{1}{s^p}\left(\sum_{k=0}^{m-1}\frac{\varphi^{(k)}(\eta,\,0)}{s^{2-p+k}} + A\left[-3\varphi_b(\eta,\,\epsilon)\frac{\partial\varphi_b(\eta,\,\epsilon)}{\partial\eta}\right]\right)\right] \tag{70}$$

$$\varphi(\eta,\,\epsilon) = A^{-1}\left[\frac{1}{s^p}\left(\sum_{k=0}^{m-1}\frac{\varphi^{(k)}(\eta,\,0)}{s^{2-p+k}} + A\left[-2\frac{\partial^3\varphi_b(\eta,\,\epsilon)}{\partial\eta^3} - 2\varphi_a(\eta,\,\epsilon)\frac{\partial\varphi_b(\eta,\,\epsilon)}{\partial\eta} - \varphi_b(\eta,\,\epsilon)\frac{\partial\varphi_a(\eta,\,\epsilon)}{\partial\eta}\right]\right)\right] \tag{71}$$

By using the Aboodh transform iteratively, the following equation is obtained:

$$\varphi_{a0}(\eta,\,\epsilon) = A^{-1}\left[\frac{1}{s^p}\left(\sum_{k=0}^{m-1}\frac{\varphi_a^{(k)}(\eta,\,0)}{s^{2-p+k}}\right)\right] = A^{-1}\left[\frac{\varphi_a(\eta,\,0)}{s^2}\right]$$

$$= \frac{3c}{2}\,\mathrm{sech}^2\left(\sqrt{\frac{c}{2}}\,\eta\right),$$

$$\varphi_{b0}(\eta,\,\epsilon) = A^{-1}\left[\frac{1}{s^p}\left(\sum_{k=0}^{m-1}\frac{\varphi_b^{(k)}(\eta,\,0)}{s^{2-p+k}}\right)\right] = A^{-1}\left[\frac{\varphi_b(\eta,\,0)}{s^2}\right]$$
$$= c\ \mathrm{sech}\left(\sqrt{\frac{c}{2}}\eta\right),$$

Applying RL integral to equations (64) and (65), we get the equivalent form

$$\varphi_a(\eta,\,\epsilon) = \frac{3c}{2}\,\mathrm{sech}^2\left(\sqrt{\frac{c}{2}}\eta\right) + A\left[-3\varphi_b(\eta,\,\epsilon)\frac{\partial\varphi_b(\eta,\,\epsilon)}{\partial\eta}\right] \tag{72}$$

$$\varphi_b(\eta,\,\epsilon) = c\ \mathrm{sech}\left(\sqrt{\frac{c}{2}}\eta\right) + A\left[-2\frac{\partial^3\varphi_b(\eta,\,\epsilon)}{\partial\eta^3} - 2\varphi_a(\eta,\,\epsilon)\frac{\partial\varphi_b(\eta,\,\epsilon)}{\partial\eta} - \varphi_b(\eta,\,\epsilon)\frac{\partial\varphi_a(\eta,\,\epsilon)}{\partial\eta}\right] \tag{73}$$

According to NITM procedure, we get the following few terms

$$\begin{aligned}
\varphi_{a0}(\eta,\,\epsilon) &= \frac{3c}{2}\,\mathrm{sech}^2\left(\sqrt{\frac{c}{2}}\eta\right),\\
\varphi_{b0}(\eta,\,\epsilon) &= c\ \mathrm{sech}\left(\sqrt{\frac{c}{2}}\eta\right),\\
\varphi_{a1}(\eta,\,\epsilon) &= \frac{3c^{5/2}\epsilon^p\tanh\left(\frac{\sqrt{c}\eta}{\sqrt{2}}\right)\mathrm{sech}^2\left(\frac{\sqrt{c}\eta}{\sqrt{2}}\right)}{\sqrt{2}p\Gamma(p)},\\
\varphi_{b1}(\eta,\,\epsilon) &= \frac{c^{5/2}\epsilon^p\tanh\left(\frac{\sqrt{c}\eta}{\sqrt{2}}\right)\mathrm{sech}\left(\frac{\sqrt{c}\eta}{\sqrt{2}}\right)}{\sqrt{2}\Gamma(p+1)},\\
\varphi_{a2}(\eta,\,\epsilon) &= \frac{3}{4}c^4\epsilon^{2p}\,\mathrm{sech}^4\left(\frac{\sqrt{c}\eta}{\sqrt{2}}\right)\left(\frac{c^{3/2}2^{2p-\frac{1}{2}}\epsilon^p\Gamma\left(p+\frac{1}{2}\right)\left(\sinh\left(\sqrt{2}\sqrt{c}\eta\right) - 4\tanh\left(\frac{\sqrt{c}\eta}{\sqrt{2}}\right)\right)}{\sqrt{\pi}\Gamma(p+1)\Gamma(3p+1)}\right.\\
&\quad\left.+\frac{2(\cosh\left(\sqrt{2}\sqrt{c}\eta\right) - 2)}{\Gamma(2p+1)}\right),\\
\varphi_{b2}(\eta,\,\epsilon) &= \frac{1}{4}c^4\epsilon^{2p}\,\mathrm{sech}^3\left(\frac{\sqrt{c}\eta}{\sqrt{2}}\right)\left(\frac{3c^{3/2}2^{2p+\frac{1}{2}}\epsilon^p\Gamma\left(p+\frac{1}{2}\right)\left(\sinh\left(\frac{3\sqrt{c}\eta}{\sqrt{2}}\right) - 6\sinh\left(\frac{\sqrt{c}\eta}{\sqrt{2}}\right)\right)\mathrm{sech}^3\left(\frac{\sqrt{c}\eta}{\sqrt{2}}\right)}{\sqrt{\pi}\Gamma(p+1)\Gamma(3p+1)}\right.\\
&\quad\left.+\frac{\cosh\left(\sqrt{2}\sqrt{c}\eta\right) - 3}{\Gamma(2p+1)}\right).
\end{aligned} \tag{74}$$

By NITM algorithm final solution is under

$$\varphi_a(\eta,\,\epsilon) = \varphi_{a0}(\eta,\,\epsilon) + \varphi_{a1}(\eta,\,\epsilon) + \varphi_{a2}(\eta,\,\epsilon) + \cdots. \tag{75}$$

$$\varphi_b(\eta,\,\epsilon) = \varphi_{b0}(\eta,\,\epsilon) + \varphi_{b1}(\eta,\,\epsilon) + \varphi_{b2}(\eta,\,\epsilon) + \cdots. \tag{76}$$

$$\begin{aligned}
\varphi_a(\eta,\,\epsilon) &= \frac{3}{2}c\,\mathrm{sech}^2\left(\frac{\sqrt{c}\eta}{\sqrt{2}}\right) + \frac{3c^{5/2}\epsilon^p\tanh\left(\frac{\sqrt{c}\eta}{\sqrt{2}}\right)\mathrm{sech}^2\left(\frac{\sqrt{c}\eta}{\sqrt{2}}\right)}{\sqrt{2}p\Gamma(p)}\\
&+\frac{3}{4}c^4\epsilon^{2p}\,\mathrm{sech}^4\left(\frac{\sqrt{c}\eta}{\sqrt{2}}\right)\left(\frac{c^{3/2}2^{2p-\frac{1}{2}}\epsilon^p\Gamma\left(p+\frac{1}{2}\right)\left(\sinh\left(\sqrt{2}\sqrt{c}\eta\right) - 4\tanh\left(\frac{\sqrt{c}\eta}{\sqrt{2}}\right)\right)}{\sqrt{\pi}\Gamma(p+1)\Gamma(3p+1)}\right.\\
&\left.+\frac{2(\cosh\left(\sqrt{2}\sqrt{c}\eta\right) - 2)}{\Gamma(2p+1)}\right) + \cdots.
\end{aligned} \tag{77}$$

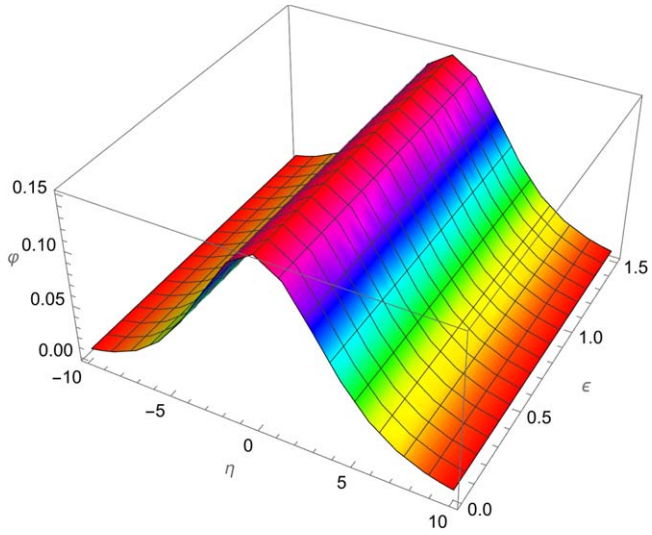

Figure 7. NITM solution $\varphi_a(\eta, \epsilon)$ for $p = 1.0$ and $\epsilon = 1.5$.

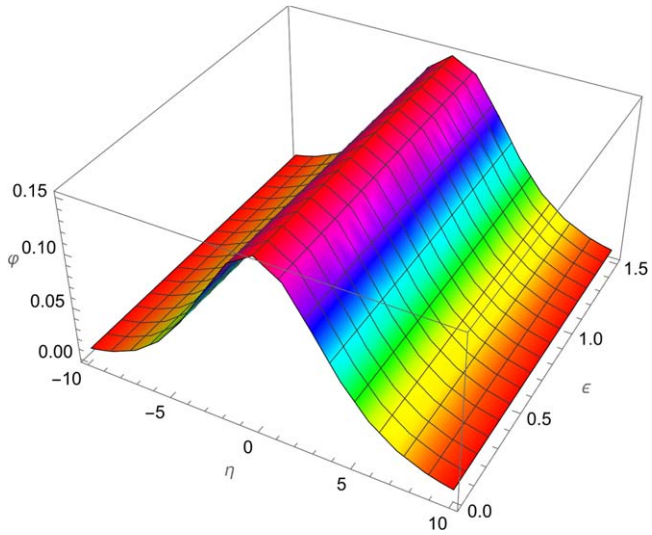

Figure 8. Exact solution $\varphi_a(\eta, \epsilon)$ at $\epsilon = 1.5$.

$$\varphi_b(\eta,\ \epsilon) = c\,\mathrm{sech}\left(\frac{\sqrt{c}\,\eta}{\sqrt{2}}\right) + \frac{c^{5/2}\epsilon^p \tanh\left(\frac{\sqrt{c}\,\eta}{\sqrt{2}}\right)\mathrm{sech}\left(\frac{\sqrt{c}\,\eta}{\sqrt{2}}\right)}{\sqrt{2}\,\Gamma(p+1)}$$
$$+\frac{1}{4}c^4\epsilon^{2p}\,\mathrm{sech}^3\left(\frac{\sqrt{c}\,\eta}{\sqrt{2}}\right)\left(\frac{3c^{3/2}2^{2p+\frac{1}{2}}\epsilon^p\Gamma\left(p+\frac{1}{2}\right)\left(\sinh\left(\frac{3\sqrt{c}\,\eta}{\sqrt{2}}\right)-6\sinh\left(\frac{\sqrt{c}\,\eta}{\sqrt{2}}\right)\right)\mathrm{sech}^3\left(\frac{\sqrt{c}\,\eta}{\sqrt{2}}\right)}{\sqrt{\pi}\,\Gamma(p+1)\Gamma(3p+1)}\right.$$
$$\left.+\frac{\cosh\left(\sqrt{2}\,\sqrt{c}\,\eta\right)-3}{\Gamma(2p+1)}\right)+\cdots. \tag{78}$$

Figure 7 displays the solution $\varphi_a(\eta, \epsilon)$ obtained using the NITM method for $p = 1.0$ and $\epsilon = 1.5$. In contrast, figure 8 exhibits the exact solution $\varphi_a(\eta, \epsilon)$ at $\epsilon = 1.5$. Figure 9 provides a comparative analysis between the NITM solution and the exact solution $\varphi_a(\eta, \epsilon)$ for $\epsilon = 1.5$. The comparison elucidates the closeness or deviation between the NITM-derived solution and the exact solution, offering insights into the accuracy of the method for this specific scenario. Similarly, figures 10, 11, and 12 depict the NITM solution $\varphi_b(\eta, \epsilon)$, the exact solution $\varphi_b(\eta, \epsilon)$ at $\epsilon = 1.5$, and the comparison of both solutions, respectively, for $p = 1.0$. These figures provide an analogous

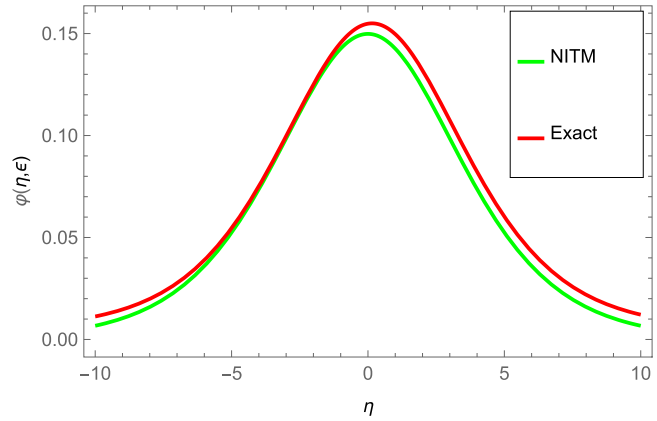

Figure 9. Comparison of exact and NITM solution $\varphi_a(\eta, \epsilon)$ at $\epsilon = 1.5$.

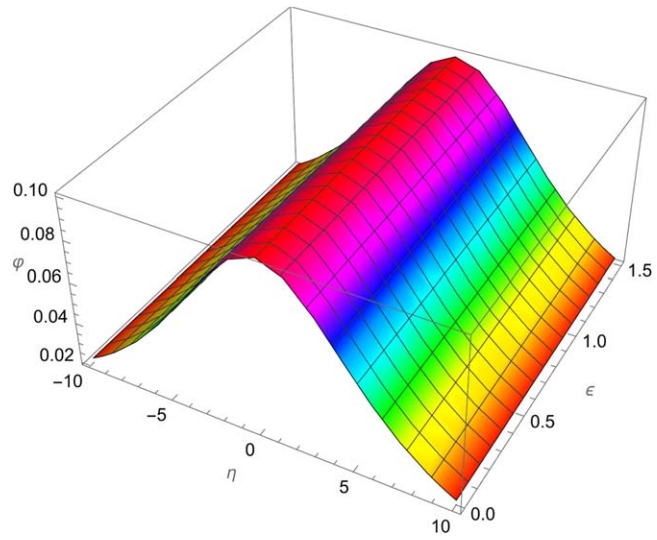

Figure 10. NITM solution $\varphi_b(\eta, \epsilon)$ for $p = 1.0$ and $\epsilon = 1.5$.

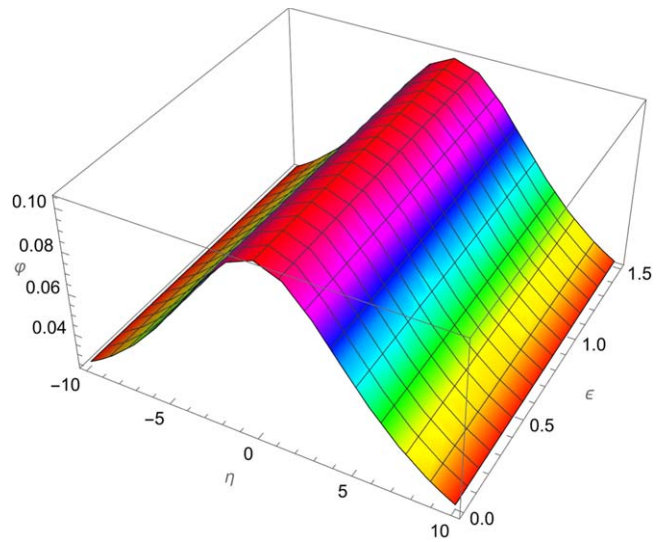

Figure 11. Exact solution $\varphi_b(\eta, \epsilon)$ at $\epsilon = 1.5$.

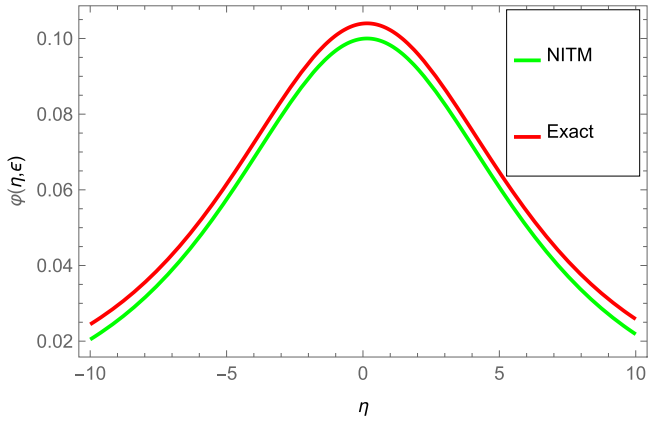

Figure 12. Comparison of exact and NITM solution $\varphi_b(\eta, \epsilon)$ at $\epsilon = 1.5$.

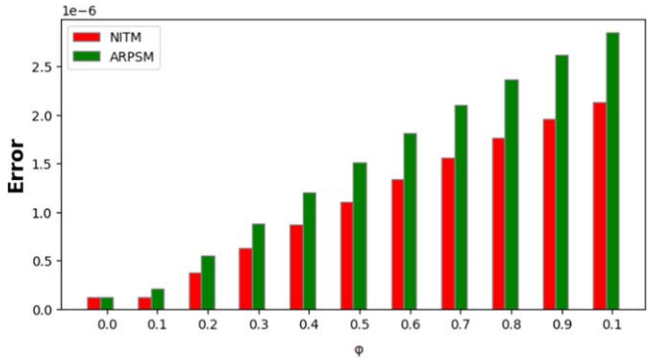

Figure 13. Comparison of absolute error for $\varphi_a(\eta, \epsilon)$ at $\epsilon = 1.5$.

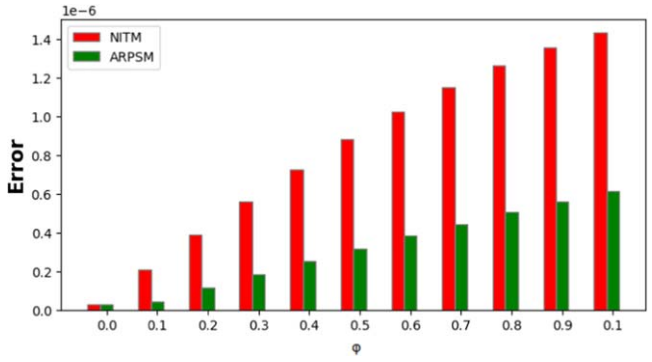

Figure 14. Comparison of absolute error for $\varphi_b(\eta, \epsilon)$ at $\epsilon = 1.5$.

comparative analysis to the previous set, focusing on a different variable or parameter within the system, shedding light on the accuracy of the NITM method for another aspect of the problem. Figures 13 and 14 present the comparison of absolute errors for $\varphi_a(\eta, \epsilon)$ and $\varphi_b(\eta, \epsilon)$, respectively, at $\epsilon = 1.5$. These figures showcase the deviations or differences between the NITM-derived solutions and the exact solutions in terms of absolute errors. Analyzing these plots allows for an understanding of the accuracy and precision of the NITM method in approximating the exact solutions.

Tables 3 and 4 provide a comprehensive comparison of different fractional orders of the NITM solutions $\varphi_a(\eta, \epsilon)$ and $\varphi_b(\eta, \epsilon)$, respectively, for $\epsilon = 1.5$ and $c = 0.1$. These tables present a systematic overview of how

Table 3. The comparison of different fractional order of NITM solution $\varphi_a(\eta, \epsilon)$ for $\epsilon = 1.5$ and $c = 0.1$.

η	$NITM_{P=0.6}$	$NITM_{p=0.8}$	$NITM_{P=1.0}$	*Exact*	$Error_{p=0.6}$	$Error_{p=0.8}$	$Error_{p=1.0}$
0.	0.149 779	0.149 799	0.149 831	0.149 831	0.000 052 837 4	0.000 032 107 9	1.264818×10^{-7}
0.1	0.149 918	0.149 947	0.149 981	0.149 981	0.000 063 401 9	0.000 034 055 6	1.265208×10^{-7}
0.2	0.149 908	0.149 945	0.149 982	0.149 981	0.000 073 713 8	0.000 035 867 7	3.785758×10^{-7}
0.3	0.149 748	0.149 794	0.149 832	0.149 831	0.000 083 734	0.000 037 538 9	6.276754×10^{-7}
0.4	0.149 439	0.149 493	0.149 533	0.149 532	0.000 093 426 3	0.000 039 064 6	8.718533×10^{-7}
0.5	0.148 982	0.149 045	0.149 086	0.149 085	0.000 102 757	0.000 040 441 9	1.109212×10^{-6}
0.6	0.148 38	0.148 45	0.148 493	0.148 491	0.000 111 695	0.000 041 668 8	1.337950×10^{-6}
0.7	0.147 634	0.147 711	0.147 755	0.147 754	0.000 120 213	0.000 042 744 3	1.556383×10^{-6}
0.8	0.146 747	0.146 832	0.146 877	0.146 875	0.000 128 287	0.000 043 668 9	1.762970×10^{-6}
0.9	0.145 723	0.145 815	0.145 861	0.145 859	0.000 135 895	0.000 044 443 9	1.956327×10^{-6}
1.	0.144 566	0.144 664	0.144 711	0.144 709	0.000 143 021	0.000 045 071 7	2.135244×10^{-6}

Table 4. The comparison of different fractional order of NITM solution $\varphi_b(\eta, \epsilon)$ for $\epsilon = 1.5$ and $c = 0.1$.

η	$NITM_{P=0.6}$	$NITM_{p=0.8}$	$NITM_{P=1.0}$	*Exact*	$Error_{p=0.6}$	$Error_{p=0.8}$	$Error_{p=1.0}$
0.	0.099 926 2	0.099 933 1	0.099 943 8	0.099 943 8	0.000 017 596 6	0.000 010 686 8	2.635513×10^{-8}
0.1	0.099 972 2	0.099 982 1	0.099 993 5	0.099 993 8	0.000 021 515 2	0.000 011 678 3	2.086800×10^{-7}
0.2	0.099 968 4	0.099 981 1	0.099 993 4	0.099 993 8	0.000 025 376 5	0.000 012 637 5	3.881233×10^{-7}
0.3	0.099 914 6	0.099 930 2	0.099 943 2	0.099 943 8	0.000 029 167 5	0.000 013 559 3	5.620196×10^{-7}
0.4	0.099 811 1	0.099 829 5	0.099 843 2	0.099 844	0.000 032 876	0.000 014 438 8	7.278125×10^{-7}
0.5	0.099 658	0.099 679 3	0.099 693 6	0.099 694 5	0.000 036 490 3	0.000 015 271 4	8.831037×10^{-7}
0.6	0.099 455 9	0.099 479 8	0.099 494 9	0.099 495 9	0.000 039 999 5	0.000 016 053 2	1.025698×10^{-6}
0.7	0.099 205 1	0.099 231 7	0.099 247 3	0.099 248 5	0.000 043 393 5	0.000 016 780 7	1.153645×10^{-6}
0.8	0.098 906 3	0.098 935 5	0.098 951 7	0.098 953	0.000 046 663 4	0.000 017 450 9	1.265269×10^{-6}
0.9	0.098 560 2	0.098 592	0.098 608 7	0.098 61	0.000 049 801 1	0.000 018 061 5	1.359200×10^{-6}
1.	0.098 167 7	0.098 201 9	0.098 219 1	0.098 220 5	0.000 052 799 7	0.000 018 610 7	1.434386×10^{-6}

Table 5. The comparison of absolute error for $\epsilon = 1.5$ of ARPSM and NITM solution $\varphi_a(\eta, \epsilon)$.

η	Exact	$NITM_{p=1.0}$	$ARPSM_{P=1.0}$	$NITMError_{p=1.0}$	$ARPSMError_{p=1.0}$
0.	0.149 831	0.149 831	0.149 831	1.264818×10^{-7}	1.264818×10^{-7}
0.1	0.149 981	0.149 981	0.149 981	1.265208×10^{-7}	2.107553×10^{-7}
0.2	0.149 981	0.149 982	0.149 982	3.785758×10^{-7}	5.462043×10^{-7}
0.3	0.149 831	0.149 832	0.149 832	6.276754×10^{-7}	8.770298×10^{-7}
0.4	0.149 532	0.149 533	0.149 533	8.718533×10^{-7}	1.200463×10^{-6}
0.5	0.149 085	0.149 086	0.149 087	1.109212×10^{-6}	1.513842×10^{-6}
0.6	0.148 491	0.148 493	0.148 493	1.337950×10^{-6}	1.814650×10^{-6}
0.7	0.147 754	0.147 755	0.147 756	1.556383×10^{-6}	2.100546×10^{-6}
0.8	0.146 875	0.146 877	0.146 878	1.762970×10^{-6}	2.369398×10^{-6}
0.9	0.145 859	0.145 861	0.145 862	1.956327×10^{-6}	2.619308×10^{-6}
1.	0.144 709	0.144 711	0.144 712	2.135244×10^{-6}	2.848634×10^{-6}

varying fractional orders impact the solutions obtained through the NITM method, allowing for an assessment of the sensitivity of solutions to changes in fractional order parameters. Tables 5 and 6 offer a comparison of the absolute errors between the ARPSM and NITM solutions $\varphi_a(\eta, \epsilon)$ and $\varphi_b(\eta, \epsilon)$, respectively, at $\epsilon = 1.5$. These tables facilitate a direct comparison between two different methods, highlighting their accuracies and potential discrepancies in approximating the exact solutions for the given scenario. In summary, the graphical figures and tables collectively provide a detailed insight into the accuracy, precision, and sensitivity of the NITM and ARPSM methods in approximating solutions for $\varphi_a(\eta, \epsilon)$ and $\varphi_b(\eta, \epsilon)$ under varying fractional orders and specific parameter settings, enhancing our understanding of the numerical solutions derived for this complex mathematical system.

Table 6. The comparison of absolute error for $\epsilon = 1.5$ of ARPSM and NITM solution $\varphi_b(\eta, \epsilon)$.

η	Exact	$NITM_{p=1.0}$	$ARPSM_{P=1.0}$	$NITMError_{p=1.0}$	$ARPSMError_{p=1.0}$
0.	0.099 943 8	0.099 943 8	0.099 943 8	2.635513×10^{-8}	2.635513×10^{-8}
0.1	0.099 993 8	0.099 993 5	0.099 993 8	2.086800×10^{-7}	4.391807×10^{-8}
0.2	0.099 993 8	0.099 993 4	0.099 993 9	3.881233×10^{-7}	1.139237×10^{-7}
0.3	0.099 943 8	0.099 943 2	0.099 944	5.620196×10^{-7}	1.832369×10^{-7}
0.4	0.099 844	0.099 843 2	0.099 844 2	7.278125×10^{-7}	2.514403×10^{-7}
0.5	0.099 694 5	0.099 693 6	0.099 694 8	8.831037×10^{-7}	3.181293×10^{-7}
0.6	0.099 495 9	0.099 494 9	0.099 496 3	1.025698×10^{-6}	3.829159×10^{-7}
0.7	0.099 248 5	0.099 247 3	0.099 248 9	1.153645×10^{-6}	4.454334×10^{-7}
0.8	0.098 953	0.098 951 7	0.098 953 5	1.265269×10^{-6}	5.053397×10^{-7}
0.9	0.098 61	0.098 608 7	0.098 610 6	1.359200×10^{-6}	5.623208×10^{-7}
1.	0.098 220 5	0.098 219 1	0.098 221 2	1.434386×10^{-6}	6.160938×10^{-7}

4. Conclusion

In conclusion, we have successfully employed the Aboodh transform iteration method and the Aboodh residual power series method to solve a fractional-order system of the Drinfeld-Sokolov-Wilson equation within the Caputo operator framework. Through our analysis and numerical experiments, we have demonstrated the accuracy and reliability of these methods in obtaining solutions for this particular system. The results not only provide a valuable contribution to the field of fractional calculus but also enhance our understanding of the behavior and dynamics of the Drinfeld-Sokolov-Wilson equation in the fractional-order context. These findings open up opportunities for further research and applications in related areas of science and mathematics.

Acknowledgments

The authors extend their appreciation to the Deanship of Scientific Research at King Khalid University for funding this work through the Small Group Research Project under grant number RGP1/216/44. This work was supported by the Deanship of Scientific Research, the Vice Presidency for Graduate Studies and Scientific Research, King Faisal University, Saudi Arabia (Grant No. 5355).

Data availability statement

The data cannot be made publicly available upon publication because they are not available in a format that is sufficiently accessible or reusable by other researchers. The data that support the findings of this study are available upon reasonable request from the authors.

ORCID iDs

Humaira Yasmin https://orcid.org/0000-0003-0199-6850
Rasool Shah https://orcid.org/0000-0002-9798-9868

References

[1] El-Mesady A I, Hamed Y S and Alsharif A M 2021 Jafari transformation for solving a system of ordinary differential equations with medical application *Fractal and Fractional* **5** 130
[2] Alhazmi S E, Abdelmohsen S A, Alyami M A, Ali A and Asamoah J K K 2022 A novel analysis of generalized perturbed zakharov-kuznetsov equation of fractional-order arising in dusty plasma by natural transform decomposition method *J. Nanomater.* 2022
[3] El-Mesady A, Elsonbaty A and Adel W 2022 On nonlinear dynamics of a fractional order monkeypox virus model *Chaos, Solitons Fractals* **164** 112716
[4] Ali A, Zada L and Nawaz R 2022 Approximate Solution of Generalized Modified b-Equation by Optimal Auxiliary Function Method *International Journal of Emerging Multidisciplinaries: Mathematics* **1** 102–10
[5] Ali A, Ullah S and Khan M A 2022 The impact of vaccination on the modeling of COVID-19 dynamics: a fractional order model *Nonlinear Dyn.* **110** 3921–40
[6] Allehiany F M, Alqahtani A M, Bilal M, Ali A and Eldin S M 2023 Fractional study of radiative Brinkman-type nanofluid flow across a vertical plate with the effect of Lorentz force and Newtonian heating *AIP Adv.* **13** 6
[7] Oldham K B 2010 Fractional differential equations in electrochemistry *Adv. Eng. Software* **41** 9–12
[8] Kbiri Alaoui M, Nonlaopon K, Zidan A M and Khan A 2022 Analytical investigation of fractional-order Cahn-Hilliard and gardner equations using two novel techniques *Mathematics* **10** 1643

[9] Botmart T, Agarwal R P, Naeem M and Khan A 2022 On the solution of fractional modified Boussinesq and approximate long wave equations with non-singular kernel operators *AIMS Math* **7** 12483–513
[10] Scalas E, Gorenflo R and Mainardi F 2000 Fractional calculus and continuous-time finance *Physica* A **284** 376–84
[11] Mukhtar S, Shah R and Noor S 2022 The numerical investigation of a fractional-order multi-dimensional Model of Navier-Stokes equation via novel techniques *Symmetry* **14** 1102
[12] Weiss C J, van Bloemen Waanders B G and Antil H 2020 Fractional operators applied to geophysical electromagnetics *Geophys. J. Int.* **220** 1242–59
[13] Yasmin H, Aljahdaly N H, Saeed A M and Shah R 2023 Probing families of optical soliton solutions in fractional perturbed radhakrishnan-kundu-lakshmanan model with improved versions of extended direct algebraic method *Fractal and Fractional* **7** 512
[14] Kumar D, Singh J and Baleanu D 2017 A hybrid computational approach for Klein-Gordon equations on Cantor sets *Nonlinear Dyn.* **87** 511–7
[15] Yasmin H, Aljahdaly N H, Saeed A M and Shah R 2023 Investigating families of soliton solutions for the complex structured coupled fractional biswas-arshed model in birefringent fibers using a novel analytical technique *Fractal and Fractional* **7** 491
[16] Bhrawy A H, Zaky M A and Baleanu D 2015 New numerical approximations for space-time fractional Burgers' equations via a Legendre spectral-collocation method *Rom. Rep. Phys* **67** 340–9
[17] Singh J, Kumar D, Hammouch Z and Atangana A 2018 A fractional epidemiological model for computer viruses pertaining to a new fractional derivative *Appl. Math. Comput.* **316** 504–15
[18] Yasmin H, Aljahdaly N H, Saeed A M and Shah R 2023 Investigating symmetric soliton solutions for the fractional coupled konno-onno system using improved versions of a novel analytical technique *Mathematics* **11** 2686
[19] Zhang W M 2011 Solitary solutions and singular periodic solutions of the Drinfeld-Sokolov-Wilson equation by variational approach *Appl. Math. Sci* **5** 1887–94
[20] Drinfeld V G and Sokolov V V 1981 Equations of Korteweg-de Vries type, and simple Lie algebras *Doklady Akademii Nauk* (Russia: Russian Academy of Sciences) vol 258, pp 11–16
[21] Drinfel'd V G and Sokolov V V 1985 Lie algebras and equations of Korteweg-de Vries type *Journal of Soviet mathematics* **30** 1975–2036
[22] Wilson G 1982 The affine Lie algebra C (1) 2 and an equation of Hirota and Satsuma *Phys. Lett.* A **89** 332–4
[23] Abdulloev K O, Bogolubsky I L and Makhankov V 1976 One more example of inelastic soliton interaction *Phys. Lett.* A **56** 427–8
[24] Bona J L, Pritchard W G and Scott L R 1985 Numerical schemes for a model for nonlinear dispersive waves *J. Comput. Phys.* **60** 167–86
[25] Benjamin T B, Bona J L and Mahony J J 1972 Model equations for long waves in nonlinear dispersive systems *Philosophical Transactions of the Royal Society of London. Series A, Mathematical and Physical Sciences* **272** 47–78
[26] Bona J L, Pritchard W G and Scott L R 1980 Solitary-wave interaction *The Physics of Fluids* **23** 438–41
[27] Inc M 2006 On numerical doubly periodic wave solutions of the coupled Drinfeld-Sokolov-Wilson equation by the decomposition method *Appl. Math. Comput.* **172** 421–30
[28] Xue-Qin Z and Hong-Yan Z 2008 An improved f-expansion method and its application to coupled drinfeld-sokolov-wilson equation *Commun. Theor. Phys.* **50** 309
[29] Singh P K, Vishal K and Som T 2015 Solution of fractional Drinfeld-Sokolov-Wilson equation using Homotopy perturbation transform method *Applications and Applied Mathematics: An International Journal (AAM)* **10** 27
[30] Singh J, Kumar D, Baleanu D and Rathore S 2018 An efficient numerical algorithm for the fractional Drinfeld-Sokolov-Wilson equation *Appl. Math. Comput.* **335** 12–24
[31] Yang X J 2019 *General Fractional Derivatives: Theory, Methods and Applications* (Boca Raton, FL: CRC Press)
[32] Yang X J, Srivastava H M and Machado J A T 2015 A new fractional derivative without singular kernel: application to the modelling of the steady heat flow *Thermal Science* **20** 753–6
[33] Yang X J, Gao F, Tenreiro Machado J A and Baleanu D 2017 A new fractional derivative involving the normalized sinc function without singular kernel *The European Physical Journal Special Topics* **226** 3567–75
[34] Yang X J, Feng Y Y, Cattani C and Inc M 2019 Fundamental solutions of anomalous diffusion equations with the decay exponential kernel *Math. Methods Appl. Sci.* **42** 4054–60
[35] Yepez-Martinez H and Gomez-Aguilar J F 2018 Numerical and analytical solutions of nonlinear differential equations involving fractional operators with power and Mittag-Leffler kernel *Mathematical Modelling of Natural Phenomena* **13** 13
[36] Atangana A and Gomez-Aguilar J F 2018 Numerical approximation of Riemann-Liouville definition of fractional derivative: from Riemann-Liouville to Atangana-Baleanu *Numerical Methods for Partial Differential Equations* **34** 1502–23
[37] Morales-Delgado V F, Gomez-Aguilar J F, Yepez-Martinez H, Baleanu D, Escobar-Jimenez R F and Olivares-Peregrino V H 2016 Laplace homotopy analysis method for solving linear partial differential equations using a fractional derivative with and without kernel singular *Advances in Difference Equations* **2016** 1–17
[38] Atangana A and Gomez-Aguilar J F 2018 Fractional derivatives with no-index law property: application to chaos and statistics *Chaos Solitons Fractals* **114** 516–35
[39] Yokus A 2018 Comparison of Caputo and conformable derivatives for time-fractional Korteweg-de Vries equation via the finite difference method *International Journal of Modern Physics* B **32** 1850365
[40] Arqub O A 2013 Series solution of fuzzy differential equations under strongly generalized differentiability *J. Adv. Res. Appl. Math* **5** 31–52
[41] Abu Arqub O, Abo-Hammour Z, Al-Badarneh R and Momani S 2013 A reliable analytical method for solving higher-order initial value problems *Discrete Dynamics in Nature and Society* 2013
[42] Arqub O A, El-Ajou A, Zhour Z A and Momani S 2014 Multiple solutions of nonlinear boundary value problems of fractional order: a new analytic iterative technique *Entropy* **16** 471–93
[43] El-Ajou A, Arqub O A and Momani S 2015 Approximate analytical solution of the nonlinear fractional KdV-Burgers equation: a new iterative algorithm *J. Comput. Phys.* **293** 81–95
[44] Xu F, Gao Y, Yang X and Zhang H 2016 Construction of fractional power series solutions to fractional Boussinesq equations using residual power series method *Mathematical Problems in Engineering* 2016
[45] Zhang J, Wei Z, Li L and Zhou C 2019 Least-squares residual power series method for the time-fractional differential equations *Complexity* **2019** 1–15
[46] Jaradat I, Alquran M and Abdel-Muhsen R 2018 An analytical framework of 2D diffusion, wave-like, telegraph, and Burgers' models with twofold Caputo derivatives ordering *Nonlinear Dyn.* **93** 1911–22
[47] Jaradat I, Alquran M and Al-Khaled K 2018 An analytical study of physical models with inherited temporal and spatial memory *The European Physical Journal Plus* **133** 1–11

[48] Alquran M, Al-Khaled K, Sivasundaram S and Jaradat H M 2017 Mathematical and numerical study of existence of bifurcations of the generalized fractional Burgers-Huxley equation *Nonlinear Stud* **24** 235–44
[49] Zhang M F, Liu Y Q and Zhou X S 2015 Efficient homotopy perturbation method for fractional non-linear equations using Sumudu transform *Thermal. Science* **19** 1167–71
[50] Ojo G O and Mahmudov N I 2021 Aboodh transform iterative method for spatial diffusion of a biological population with fractional-order *Mathematics* **9** 155
[51] Awuya M A, Ojo G O and Mahmudov N I 2022 Solution of space-time fractional differential equations using aboodh transform iterative method *Journal of Mathematics* 2022
[52] Awuya M A and Subasi D 2021 Aboodh transform iterative method for solving fractional partial differential equation with Mittag-Leffler Kernel *Symmetry* **13** 2055
[53] Cai X, Tang R, Zhou H, Li Q, Ma S, Wang D and Zhou L 2021 Dynamically controlling terahertz wavefronts with cascaded metasurfaces *Advanced Photonics* **3** 036003
[54] Chen H, Chen W, Liu X and Liu X 2021 Establishing the first hidden-charm pentaquark with strangeness *The European Physical Journal C* **81** 409
[55] Yang R and Kai Y 2023 Dynamical properties, modulation instability analysis and chaotic behaviors to the nonlinear coupled Schrodinger equation in fiber Bragg gratings *Mod. Phys. Lett.* B 2350239
[56] Zhou X, Liu X, Zhang G, Jia L, Wang X and Zhao Z 2023 An Iterative Threshold Algorithm of Log-Sum Regularization for Sparse Problem *IEEE Trans. Circuits Syst. Video Technol.* **33** 4728–40
[57] Guo C, Hu J, Wu Y and Celikovsky S 2023 Non-singular fixed-time tracking control of uncertain nonlinear pure-feedback systems with practical state constraints *IEEE Transactions on Circuits and Systems I: Regular Papers* **70** 3746–58
[58] Li S, Chen H, Chen Y, Xiong Y and Song Z 2023 Hybrid method with parallel-factor theory, a support vector machine, and particle filter optimization for intelligent machinery failure identification *Machines* **11** 837
[59] Yin Y, Zhang R and Su Q 2023 Threat assessment of aerial targets based on improved GRA-TOPSIS method and three-way decisions *Mathematical Biosciences and Engineering* **20** 13250–66
[60] Liaqat M I, Etemad S, Rezapour S and Park C 2022 A novel analytical Aboodh residual power series method for solving linear and nonlinear time-fractional partial differential equations with variable coefficients *AIMS Mathematics* **7** 16917–48
[61] Liaqat M I, Akgul A and Abu-Zinadah H 2023 Analytical Investigation of Some Time-Fractional Black-Scholes Models by the Aboodh Residual Power Series Method *Mathematics* **11** 276
[62] Aboodh K S 2013 The New Integral Transform'Aboodh Transform *Global journal of pure and Applied mathematics* **9** 35–43
[63] Aggarwal S and Chauhan R 2019 A comparative study of Mohand and Aboodh transforms *International journal of research in advent Technology* **7** 520–9
[64] Benattia M E and Belghaba K 2020 Application of the Aboodh transform for solving fractional delay differential equations *Universal Journal of Mathematics and Applications* **3** 93–101
[65] Delgado B B and Macias-Diaz J E 2021 On the general solutions of some non-homogeneous Div-curl systems with Riemann-Liouville and Caputo fractional derivatives *Fractal and Fractional* **5** 117
[66] Alshammari S, Al-Smadi M, Hashim I and Alias M A 2019 Residual power series technique for simulating fractional bagley-torvik problems emerging in applied physics *Applied Sciences* **9** 5029